Pausing Model Learning in Real-world Reinforcement Learning

Hyunin Lee [1] **Ming Jin** [2] **Javad Lavaei** [1] **Somayeh Sojoudi** [1]

Abstract

Real-time inference is a challenge of real-world reinforcement learning due to temporal differences in time-varying environments: the system collects data from the past, updates the decision model in the present, and deploys it in the future. We tackle a common belief that continually updating the decision is optimal to minimize the temporal gap. We propose forecasting an online reinforcement learning framework and show that strategically pausing decision updates yields better overall performance by effectively managing aleatoric uncertainty. Theoretically, we compute an optimal ratio between policy update and hold duration and show that a non-zero policy hold duration provides a sharper upper bound on the dynamic regret. Our experimental evaluations on three different environments also reveal that a non-zero policy hold duration yields higher rewards compared to continuous decision updates.

1. Introduction

Real-world reinforcement learning (RL) bridges the gap between the current literature on RL and real-world problems. *Real-time inference*, a key challenge in real-world RL, requires that inference occur in real-time at the control frequency of the system (Dulac-Arnold et al., 2019). For RL deployment in a production system, policy inference must occur in real-time, matching the control frequency of the system. This could range from milliseconds for tasks such as recommendation systems (Covington et al., 2016; Steck et al., 2021) or autonomous vehicle control (Hester & Stone, 2013), to minutes for building control systems (Evans & Gao). This constraint prevents us from speeding up the task beyond real-time to rapidly generate extensive data (Silver et al., 2016; Espeholt et al., 2018) or slowing it down for more computationally intensive approaches (Levine et al., 2019; Schrittwieser et al., 2020). One strategy for real-time action is to employ a multi-threaded architecture, where model learning and planning occur in background threads while actions are returned in real-time (Hester & Stone, 2013; Imanberdiyev et al., 2016; Glavic et al., 2017).

In this paper, we show that intentionally pausing model learning can lead to better overall performance than continuous model updating. Our study is based on deriving an analytical solution for the optimal ratio between the pausing and updating phases. Perhaps most importantly, this paper offers the insight that the pausing phase is crucial to handling an aleatoric uncertainty that stems from the environment's intrinsic uncertainty.

This paper begins with a fundamental observation of the real-time inference mechanism based on prediction: the agent forecasts the *future* based on *past* data, and then continually updates decisions in the *present* based on future predictions. This highlights the significance of balancing conservatism or pessimism in decision-making, based on the three types of uncertainties: epistemic, aleatoric, and predictive uncertainties (Gal, 2016). We define conservatism as expecting past trends to continue in the future, and pessimism as anticipating future differences. Although accumulating extensive past data reduces aleatoric uncertainty, and a prediction model with high capacity lessens predictive uncertainty, the frequency of policy updates still remains a key factor due to unknown aleatoric uncertainty in the present.

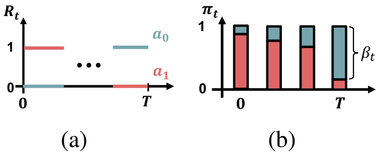

(a) (b) (c)

Figure 1. (a) Non-stationary bandit setting, (b) conservative policy, (c) pessimistic policy

To elucidate the importance of the above problem, consider a recommendation system tasked with optimally suggesting item x_0 or x_1 to a user whose preference changes over time. This can be framed as a Bernoulli non-stationary bandit setting with a set of two actions $\mathcal{A} = \{a_0, a_1\}$, and a time-dependent policy $\pi_t : \mathcal{A} \to [0, 1]$, where $\pi_t(a_0) = \beta_t$ and $\pi_t(a_1) = 1 - \beta_t$, $0 \leq \beta_t \leq 1$. The rewards of each action, denoted as R_t, switch (i.e., $R_t(a_0) \leftrightarrow R_t(a_1)$) once at an unpredictable time between 0 and T (see Figure 1 (a)). The

[1] University of California, Berkeley [2] Virginia Tech. Correspondence to: Hyunin Lee <hyunin@berkeley.edu>.

Preprint. Under review.

goal of the system is to maximize the average rewards over a period T, i.e., $\max_{\pi_1,\dots,\pi_T} \mathbb{E}\left[\sum_{t=0}^{T} R_t(a)\right]$. Initially, recommending x_1 yields a higher reward ($R_0(a_1) = 1$). However, the system anticipates a shift in user preference towards x_0 by the end of period T. The system should optimize its policy π_t during the interval from 0 to T, facing aleatoric uncertainty about when the user preferences will change. A conservative policy increases the preference weight β_t associated with x_0 too quickly (Figure 1 (b)), while a pessimistic approach may adjust too slowly (Figure 1 (c)). The key challenge is to determine the optimal tempo of policy adjustment in anticipation of this unknown preference shift.

Based on the previous example, this paper challenges the belief that continually updating the decision always achieves an optimal bound of dynamic regret, a measurement of decision optimality in a time-varying environment. Our main contribution, Algorithm 1 and Theorem 5.8, demonstrates that strategically pausing decision updates provides a sharper upper bound on the dynamic regret by deriving an optimal ratio between the policy update duration and the pause duration.

To achieve this, we formulate the online interactive learning problem in Section 3 by determining three key aspects: 1) the frequency of policy updates, 2) the timing of policy updates, and 3) the extent of each update. First, we study the real-time inference mechanism by proposing a forecasting online reinforcement learning model-free framework in Section 4. In Section 5, we calculate an upper bound on the dynamic regret (Theorem 5.3) as a function of episodic and predictive uncertainties (Propositions 4.1 and 4.2), as well as aleatoric uncertainty (Proposition 5.6 and Lemma 5.7). This is achieved by separating it into the policy update phase (Lemma 5.1) and the policy hold phase (Lemma 5.2). In Subsection 5.3, we conduct numerical experiments to show how the optimal ratio minimizing the dynamic regret's upper bound (Theorem 5.8) varies with hyperparameters related to aleatoric uncertainty, highlighting the significance of the policy hold phase in this minimization. Finally, in Section 6, we empirically show two findings from three non-stationary environments: 1) the higher average reward of the forecasting method compared to the reactive method (Subsection 6.2), and 2) the non-positive correlation relationship between update ratios and average returns (Subsection 6.3).

Notations

The sets of natural, real, and non-negative real numbers are denoted by $\mathbb{N}$, $\mathbb{R}$, and $\mathbb{R}_+$, respectively. For a finite set Z, the notation $|Z|$ represents its cardinality, and $\Delta(Z)$ denotes the probability simplex over Z. Given $X, Y \in \mathbb{N}$ with $X < Y$, we define $[X] := \{1, 2, \dots, X\}$, the closed interval $[X, Y] := \{X, X+1, \dots, Y\}$, and the half-open interval $[X, Y) := \{X, X+1, \dots, Y-1\}$. For $x \in \mathbb{R}_+$, the floor function $\lfloor x \rfloor$ is defined as $\max\{n \in \mathbb{N} \cup \{0\} \mid n \leq x\}$. For any functions $f, g : \mathbb{R}^m \to \mathbb{R}$ satisfying $f(x) \leq g(x)$ for all values of x, if $x_g^* = \arg\min_{x \in \mathbb{R}^m} g(x)$, then x_g^* is referred to as a surrogate optimal solution of $f(x)$. We use the term surrogate optimal solution and suboptimal solution interchangeably.

2. Related works

Real-time inference RL

One approach to real-time reinforcement learning is to adapt existing algorithms and validate their feasibility for real-time operation (Adam et al., 2012). Alternatively, some algorithms are specifically designed with the primary objective of functioning in real-time contexts (Cai et al., 2017; Wang & Yuan, 2015). A recent and distinct perspective on real-time inference was presented in (Ramstedt & Pal, 2019), which proposed the real-time markov reward process. In this process, the state evolves concurrently with the action selection. The anytime inference approach (Vlasselaer et al., 2015; Spirtes, 2001) encompasses a set of algorithms capable of returning a valid solution at any interruption point, with their performance improving over time.

Nonstationary RL

The problem formulation of this paper draws inspiration from "desynchronized-time environment", initially proposed by (Lee et al., 2023). The desynchronized-time environment assigns the real-time duration of the learning process, where the agent is responsible for deciding both the timing and the duration of its interactions. (Finn et al., 2019) introduced the Follow-The-Meta-Leader algorithm to improve parameter initialization in a non-stationary environment, but it cannot efficiently handle delays in optimal policy tracking. To address this, (Chandak et al., 2020b;a) developed methods for forecasting policy evaluation, yet faced limitations in empirical analysis and theoretical bounds for policy performance. (Mao et al., 2021) proposed an adaptive Q-learning approach with a restart strategy, establishing a near-optimal dynamic regret bound.

3. Problem Statement

Time-elapsing Markov Decision Process (Lee et al., 2023). For a given time $t \in [0, T]$, we define the Markov Decision Process (MDP) at time t as $\mathcal{M}_t := \langle \mathcal{S}, \mathcal{A}, P_t, R_t, \gamma, H \rangle$. $\mathcal{S}$ is a state space, $\mathcal{A}$ is an action space, $P_t : \mathcal{S} \times \mathcal{A} \times \mathcal{S} \to \Delta(\mathcal{S})$ is a transition probability at time t, and $R_t : \mathcal{S} \times \mathcal{A} \to \mathbb{R}$ is a reward function at time t. For every time t, the agent interacts with the environment via a policy $\pi_t : \mathcal{S} \times \mathcal{A} \to \Delta(\mathcal{S})$ where each episode takes H steps to complete. We assume that a trajectory is finished within a second, implying that the agent will finish its trajectory within a temporally fixed MDP $\mathcal{M}_t$.

Time elapsing variation budget. In the real world, the time of the environment flows independently from $t = 0$ to $t = T$ regardless of the agent's behavior. For any time instances $t_1, t_2 \in [0, T)$ such that $t_1 < t_2$, we define *local variation budgets* $B_r(t_1, t_2)$ and $B_p(t_1, t_2)$ as

$$B_r(t_1, t_2) \coloneqq \sum_{t=t_1}^{t_2-1} \max_{s,a} |R_{t+1}(s, a) - R_t(s, a)| \,,$$
$$B_p(t_1, t_2) \coloneqq \sum_{t=t_1}^{t_2-1} \max_{s,a} ||P_{t+1}(\cdot \mid s, a) - P_t(\cdot \mid s, a)||_1 \,.$$

Also, we define *cumulative variation budgets* $\bar{B}_p(t_1, t_2)$ and $\bar{B}_r(t_1, t_2)$ as the summation of local variation budgets between time t_1 and t_2, i.e,

$$\bar{B}_r(t_1, t_2) \coloneqq \sum_{t=t_1}^{t_2-1} B_r(t_1, t), \bar{B}_p(t_1, t_2) \coloneqq \sum_{t=t_1}^{t_2-1} B_p(t_1, t).$$

To align with real-world scenarios where environmental changes do not normally occur too abruptly, we propose that these changes follow an exponential growth.

Assumption 3.1 (Exponential order local variation budget)**.** *For any time interval $[t_1, t_2] \subset [0, T)$, there exist constants $k_r, k_p > 1, B_p^{max}, B_r^{max} > 0$ such that $B_p(t_1, t) \leq B_p^{max} k_p^{t-t_1}$, $B_r(t_1, t) \leq B_r^{max} k_r^{t-t_1}$ hold for $\forall t \in [t_1, t_2]$.*

Building on Assumption 3.1, we will derive cumulative variation budgets that also adhere to an exponential order.

Corollary 3.2 (Exponential order cumulative variation budget)**.** *For arbitrary time instances $t_1, t_2 \in [0, T)$ satisfying $t_1 < t_2$, there exist constants $\alpha_r, \alpha_p > 1$ such that $\bar{B}_p(t_1, t_2) \leq B_p^{max} \alpha_p^{t_2-t_1}$, $\bar{B}_r(t_1, t_2) \leq B_r^{max} \alpha_r^{t_2-t_1}$ hold.*

Next, we define stationary and non-stationary environments in context of variation budget.

Definition 3.3 (Stationary environment)**.** *For arbitrary time instances $t_1, t_2 \in [0, T]$, if $B_r(t_1, t_2) = 0$ and $B_p(t_1, t_2) = 0$ are satisfied, then we call the corresponding environment a stationary environment.*

Definition 3.4 (Non-stationary environment)**.** *If there exist $t_1, t_2 \in [0, T]$ such that $B_r(t_1, t_2) > 0$ or $B_p(t_1, t_2) > 0$, then we call the corresponding environment a non-stationary environment.*

State value function, State action value function. For any policy π, we define the state value function $V_t^\pi : \mathcal{S} \to \mathbb{R}$ and the state action value function $Q_t^\pi : \mathcal{S} \times \mathcal{A} \to \mathbb{R}$ at time t as $V_t^\pi(s) \coloneqq \mathbb{E}_{\mathcal{M}_t}\left[\sum_{h=0}^{H-1} \gamma^h r_{t,h} \mid s_t^0 = s\right]$ and $Q_t^\pi(s, a) \coloneqq \mathbb{E}_{\mathcal{M}_t}\left[\sum_{h=0}^{H-1} \gamma^h r_{t,h} \mid s_t^0 = s, a_t^0 = a\right]$, where $r_{t,h} \coloneqq R_t(s_t^h, a_t^h)$. We define the optimal policy at time t as $\pi_t^* = \arg\max_\pi V_t^\pi$.

Dynamic regret. During the interval $[0, T]$, the agent operates according to a sequence of policies $\pi_1, \pi_2, \ldots, \pi_T$. Drawing from the learning procedure outlined previously, we define the time-varying dynamic regret $\mathfrak{R}(T) \coloneqq \sum_{t=1}^{T} (V_t^* - V_t^{\pi_t})$, where V_t^* represents the optimal policy value at time t and $V_t^{\pi_t}$ is the value function obtained by executing policy π_t in the MDP $\mathcal{M}_t$.

Parallel process of policy learning and data collection. In our formalization of a real-world learning environment, the policy learning phase and the data collection phase (interaction) occur concurrently. In this context, the number of trajectories an agent can execute between the unit times $(t, t+1), \forall t \in [T-1]$, typically depends on the system's control frequency or its hardware capabilities. However, for the purposes of our analysis, we assume that the agent executes one trajectory per unit time. This means that at time t, the agent has rolled out a total of t trajectories.

Before the first episode, the agent determines several key parameters:

1. **Frequency of Policy Updates:** The agent decides on the number of updates, denoted as $M \in \mathbb{N}$ times.
2. **Timing of Policy Updates:** The update times are set as a sequence $\{t_1, t_2, t_3, \ldots, t_M\}$ within $[0, T]$.
3. **Extent of Each Update:** The policy update iteration sequence is defined as $\{G_1, G_2, \ldots, G_M\}$.

Specifically, at each time $t_m \in [0, T]$ where $m \in [M]$, the agent updates its policy for $G_m \in \mathbb{N} \cup \{0\}$ iterations, using all previously collected trajectories. We assume that each policy iteration corresponds to one second in real-time. The policy then remains fixed for $N_m \in \mathbb{N} \cup \{0\}$ seconds after the updates, where it is determined as $N_m = t_{m+1} - (t_m + G_m)$. The next episode starts immediately at time $t_{m+1} = t_m + G_m + N_m$. Without loss of generality, we assume that $t_1 = 0$, and therefore $t_m = \sum_{i=1}^{m-1}(N_i + G_i)$ holds. Also, we define the m^{th} policy update interval as $\mathcal{G}_m \coloneqq [t_m, t_m + G_m)$ and the m^{th} policy hold interval as $\mathcal{N}_m \coloneqq [t_m + G_m, t_{m+1})$. For simplicity of notation, we denote $\bar{B}_r(t_m, t_m + G_m)$, $\bar{B}_r(t_m + G_m, t_{m+1})$, $\bar{B}_p(t_m, t_m + G_m)$ and $\bar{B}_p(t_m + G_m, t_{m+1})$ as $\bar{B}_r(\mathcal{G}_m)$, $\bar{B}_r(\mathcal{N}_m)$, $\bar{B}_p(\mathcal{G}_m)$ and $\bar{B}_p(\mathcal{N}_m)$, respectively.

How to determine $\{\pi_1, \pi_2, \ldots, \pi_T\}$. At time t_m, the agent executes the policy π_{t_m} and starts optimizing the policy for G_m seconds. During this optimization, after g iterations (seconds), where $g \in [G_m]$, the agent executes the most recently updated policy $\pi_{t_m}^g$. This updated policy represents the g^{th} iteration of optimization from the initial policy π_{t_m}. Therefore, during the policy update interval $\mathcal{G}_m$, specifically at time $t_m + g$, the policy π_{t_m+g} is equivalent to $\pi^g_{t_m}$. Subsequently, throughout the policy hold interval $\mathcal{N}_m$, the agent continues to execute the latest updated policy, denoted as $\pi_t = \pi^{G_m}_{t_m}$ for every t within $\mathcal{N}_m$.

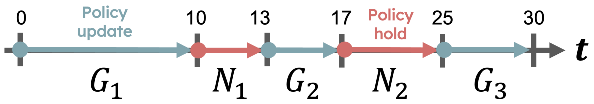

Figure 2. Parallel process of policy learning and data collection.

Example. Figure 2 illustrates our problem setting. For a given time duration between $t = 0$ and $t = 30$, suppose that the agent has chosen a frequency of policy updates as $M = 3$ and an update time sequence as $t_1 = 0, t_2 = 13, t_3 = 25$, along with policy update durations $G_1 = 10, G_2 = 4, G_3 = 5$. The agent begins the first episode at $t = 0$ with a random policy π_0. Subsequently, during times $t = 1, 2, \ldots, 10$, the agent executes continuously updating policies $\pi^1_0, \pi^2_0, \ldots, \pi^{10}_0$, respectively, and then employs the latest updated policy π^{10}_0 at times $t = 11, 12, 13$. Following this, the agent operates with policies $\pi^1_{13}, \pi^2_{13}, \ldots, \pi^4_{13}$ during the period $t = 14, 15, 16, 17$, where $\pi_{13} = \pi^{10}_0$. Lastly, it executes with the most recently updated policy π^4_{13} during the time $t = 18, \ldots, 25$.

4. Method

To implement a real-time inference mechanism, particularly emphasizing the prediction-based control: *"predicting the future in the past"*. We introduce a model-free proactive algorithm, detailed in Algorithm 1. This approach is based on the proactive evaluation of policies. At policy update time t_m, our proposed algorithm forecasts the future Q value of time t_{m+1} based on previous trajectories and then optimizes the future policy for duration $\mathcal{G}_m$ based on foreacasted future Q value. For all $t \in [0, T]$, we denote the estimated value of Q based on the past trajectories as $\widehat{Q}_t$ and the optimal value of Q as Q^*_t. We also denote the future Q value of time t_{m+1} which was forcasted at time t_m as $\widetilde{Q}_{t_{m+1}|t_m}$. During the time duration $\mathcal{G}_m$, we determine the policies $\{\pi^g_{t_m}\}^{G_m}_{g=1}$ by utilizing the Natural Policy Gradient (Kakade, 2001) with the entropy regularization method based on $\widetilde{Q}_{t_{m+1}|t_m}$ as follows:

$$\pi^{g+1}_{t_m}(\cdot|s) \propto \left(\pi^g_{t_m}(\cdot|s)\right)^{1-\frac{\eta\tau}{1-\gamma}} \exp\left(\frac{\eta\tilde{Q}_{t_{m+1}|t_m}}{1-\gamma}\right)$$
$$\text{s.t.} \quad ||\tilde{Q}_{t_{m+1}|t_m} - Q^*_{t_{m+1}}||_\infty = \delta^f_m$$

where η is a learning rate, τ is an entropy regularization parameter and δ^f_m is the maximum forecasting error at time step t_m.

There are various methods to forecast $Q_{t_{m+1}|t_m}$ based on past Q estimates $\{\widehat{Q}_t\}^{t_m}_{t=0}$. In this work, we provide analytical explanations on how the forecasting error can be bounded by the past l uncertainties (Q estimation errors) and the intrinsic uncertainty of the future environment (local variation budgets). For any t, we refer to ϵ_t as the maximum Q estimation error if $||\widehat{Q}_t - Q^*_t||_\infty \leq \epsilon_t$ holds. To simplify the presentation, we drop the term "maximum" when it is clear from the context.

Proposition 4.1 (Linear forecasting method with bounded l_2 norm)**.** *Consider a past reference length $l_p \in \mathbb{N}$ and define $\boldsymbol{w} := [w_{t_m-l_p+1}, \ldots, w_{t_m-1}, w_{t_m}]^\top$. We forecast $\tilde{Q}_{t_{m+1}|t_m}$ as a linear combination of the past l_p-estimated Q values, namely $\tilde{Q}_{t_{m+1}|t_m} = \sum^{t_m}_{t=t_m-l_p+1} w_t\hat{Q}_t$, where the condition $\|\boldsymbol{w}\|_2 \leq L$ holds for some L. Then, δ_m can be bounded by*

$$\delta^f_m \leq L\sqrt{\sum^{t_m}_{t=t_m-l_p+1} 2\left(\max(u_t, \epsilon_t)\right)^2 + l_p(L+1)}$$
$$\left(\frac{1-\gamma^H}{1-\gamma}r_{max}\right)$$

where $u_t := \frac{1-\gamma^H}{1-\gamma}\left(B_r(t, t_{m+1}) + \frac{r_{max}}{1-\gamma}B_p(t, t_{m+1})\right)$ and $r_{max} := \max_{t,s,a} |R_t(s, a)|$

Proposition 4.1 shows that utilizing a low-complexity forecasting model provides that the m^{th} maximum forecasting error is bounded by intrinsic environment uncertainty of future $\{u_t\}^{t_m}_{t=t_m-l_p-1}$ and past uncertainties $\{\epsilon_t\}^{t_m}_{t=t_m-l_p-1}$ due to finite samples.

Compared to previous studies on finite-time Q value convergence with asynchronous updates (Qu & Wierman, 2020; Even-Dar & Mansour, 2004), our work primarily focuses on how strategic policy update intervals affect an upper bound on the dynamic regret, leaving room for future exploration of Q convergence rate improvement. This will be discussed in more detail in Section 5.

In the remainder of this section, we investigate in Proposition 4.2 and Corollary 4.3 how an ϵ_t-accurate estimate of past Q value establishes a lower bound condition on $\{N_i\}^{m-1}_{i=1}$ and $\{G_i\}^{m-1}_{i=1}$.

Proposition 4.2 (Past uncertainty with sample complexity (Qu & Wierman, 2020))**.** *For any $\kappa > 0$ and under some conditions on stepsizes, if $t \geq \frac{(|S||A|)^{3.3}}{(1-\gamma)^{5.2}\epsilon_t^{2.6}}$, then $||\widehat{Q}_t - Q^*_t||_\infty \leq \epsilon_t$ holds.*

Proposition 4.2 highlights that the lower bound conditions of $\{N_i\}^{m-1}_{i=1}$ and $\{G_i\}^{m-1}_{i=1}$ are useful to reach ϵ_t-accurate estimate of Q value for asynchronous Q-learning method on a single trajectory. The upper bound of δ^f_m could be better minimized by taking $\max(u_t, \epsilon_t) = u_t$ for all $t \in$

Algorithm 1 Forecasting Online Reinforcement Learning

```
Input: Total time $T$, Policy update duration sets $\{H_1, .., H_M\}$, $\{G\}_{1:K}$, Dataset $\mathcal{D}$
Init: $m = 0$, $\pi_1$ = random policy
for $t = \{1, 2, ..., T\}$ do
    Rollout $H$ steps trajectory with policy $\pi_t$ and save a trajectory to $\mathcal{D}$
    if $t \in \{t_1, t_2, ..., t_M\}$ then
        $m \leftarrow m + 1$
        $\widetilde{Q}_{t_{m+1}|t_m} = \texttt{ForQ}(\mathcal{D})$ /* Forecast future Q */
    end if
    if $t \in [t_m + G_m)$ then
        $\pi_{t+1} = \texttt{Update}(\pi_t, \eta, \tau, \gamma, \widetilde{Q}_{t_{m+1}|t_m})$ /* Update Policy */
    else if $t \in [t_m + G_m + N_m)$ then
        $\pi_{t+1} = \pi_t$ /* Pause policy update*/
    end if
end for
```

$[t_m - l + 1, t_m]$. This requires $t \geq \frac{(|S||A|)^{3.3}}{(1-\gamma)^{5.2} u_t^{2.6}}$ to hold for all $t \in [t_m - l + 1, t_m]$. Note that $t_m = \sum_{i=1}^{m-1}(N_i + G_i)$ holds. Therefore, for $j = 1, 2, ..., l_p$, we have $\sum_{i=1}^{m-1}(N_i + G_i) - j + 1 \geq \frac{(|S||A|)^{3.3}}{(1-\gamma)^{5.2} u_{t_m - j+1}^{2.6}}$. Then, the upper bound can be simplified without past uncertainty terms as follows.

Corollary 4.3 (Maximum forecasting error bound)**.** *For $j = 1, 2, ..., l_p$, if $\{N_i\}_{i=1}^{m-1}$ and $\{G_i\}_{i=1}^{m-1}$ satisfy the condition $\sum_{i=1}^{m-1}(N_i + G_i) - j + 1 \geq \frac{(|S||A|)^{3.3}}{(1-\gamma)^{5.2} u_{t_m - j+1}^{2.6}}$, then δ_f is bounded by*

$$\delta_f \leq L u_{max} \sqrt{2 l_p} + l_p (L + 1) \left(\frac{1 - \gamma^H}{1 - \gamma} r_{max} \right).$$

where $\delta_f := \max_{m \in [M]} \delta_m^f$ is a maximum forecasting error and $u_{max} := \max_{m \in [M]} u_{t_m - l_p + 1}$.

Corollary 4.3 shows how the forecasting error δ_f is bounded with future environment's uncertainty u_{max} with lower bound conditions on $\{N_i\}_{i=1}^{m-1}$ and $\{G_i\}_{i=1}^{m-1}$. By collecting more trajectories per the unit time $(t, t+1)$, we can significantly relax the lower bound condition, going beyond our initial assumption (see Section 3).

5. Theoretical Analysis

In this section, we provide a dynamic regret analysis to investigate how policy hold durations $\{N_1, N_2, \ldots, N_M\}$ influence the minimization of dynamic regret. We initially decompose the regret into two main components and calculate the upper bounds of these components in Subsection 5.1. Subsequently, in Subsection 5.2, we further divide the overall upper bound of regret into three distinct terms and investigate how N_m modulates each of these terms, except for the future forecasting regret term. Finally, in Subsection 5.3, we present numerical experiments that demonstrate variations in the regret upper bound in response to different N_m values under different aleatoric uncertainties.

5.1. Regret analysis

We define the dynamic regret between times t_m and t_{m+1} as $\mathfrak{R}_m(T)$, which is given by $\mathfrak{R}_m(T) := \sum_{t=t_m}^{t_{m+1}} (V_t^* - V_t^{\pi_t})$. The m^{th} dynamic regret, $\mathfrak{R}_m(T)$, can be decomposed into the following two components, Policy update regret and Policy hold regret as follows:

$$\mathfrak{R}(T) = \sum_{m=1}^{M} \Bigg(\underbrace{\sum_{t \in \mathcal{G}_m} (V_t^* - V_t^{\pi_t})}_{\text{Policy update regret}} + \underbrace{\sum_{t \in \mathcal{N}_m} (V_t^* - V_t^{\pi_t})}_{\text{Policy hold regret}} \Bigg).$$

The policy update regret and the policy hold regret will be studied next.

Lemma 5.1 (Policy update regret)**.** *Let $\bar{B}(\mathcal{G}_m) := C_4 \bar{B}_r(\mathcal{G}_m) + C_5 \bar{B}_p(\mathcal{G}_m)$. For all $t \in \mathcal{G}_m$ where $m \in [M]$, it holds that*

$$\sum_{t \in \mathcal{G}_m} (V_t^* - V_t^{\pi_t}) \leq \frac{C_1}{\eta\tau} \cdot \Big(1 - (1 - \eta\tau)^{G_m}\Big) + G_m \Big(C_2 \delta_m^f + C_3\Big) + \bar{B}(\mathcal{G}_m)$$

where $C_1 = (\gamma + 2)\Big(||Q_{t_m}^* - Q_{t_m}||_\infty + 2\tau(1 - \frac{\eta\tau}{1-\gamma} || \log \pi_{t_m}^* - \log \pi_{t_m}||_\infty)\Big), C_2 = \frac{2(\gamma+2)}{1-\gamma}\left(1 + \frac{\gamma}{\eta\tau}\right), C_3 = \frac{2\tau \log |\mathcal{A}|}{1-\gamma}, C_4 = \frac{2(1-\gamma^H)}{1-\gamma}, C_5 = \frac{\gamma}{1-\gamma} \cdot \left(\frac{1-\gamma^H}{1-\gamma} - \gamma^{H-1} H\right) + \frac{1-\gamma^H}{1-\gamma} \cdot \frac{r_{max}}{1-\gamma}$.

Lemma 5.2 (Policy hold regret)**.** *Let $\bar{B}(\mathcal{N}_m) := C_4 \bar{B}_r(\mathcal{N}_m) + C_5 \bar{B}_p(\mathcal{N}_m)$. For all $t \in \mathcal{N}_m$ where $m \in [M]$, it holds that*

$$\sum_{t \in \mathcal{N}_m} (V_t^* - V_t^{\pi_t}) \leq N_m \cdot \Big(C_1 (1 - \eta\tau)^{G_m} + C_2 \delta_m^f + C_3\Big) + \bar{B}(\mathcal{N}_m)$$

where C_1, C_2, C_3, C_4, C_5 are the constants defined in Lemma 5.1.

By leveraging Lemmas 5.1 and 5.2, the dynamic regret $\mathfrak{R}(T)$ will be bounded below.

Theorem 5.3 (Dynamic regret)**.** *Let $\bar{B}(t_m, t_{m+1}) :=$*

$\bar{B}(\mathcal{N}_m) + \bar{B}(\mathcal{G}_m)$. *Then, it holds that*

$$\mathfrak{R}(T) \leq \sum_{m=1}^{M} \Bigg(\underbrace{\frac{C_1}{\eta\tau} + \left(N_m C_1 - \frac{C_1}{\eta\tau} \right) (1-\eta\tau)^{G_m}}_{\text{policy optimization regret}(\mathfrak{R}_m^{\pi})}$$

$$+ \underbrace{(N_m + G_m)(C_2 \delta_m^f + C_3)}_{Q\text{ function forecasting regret}(\mathfrak{R}_m^f)} + \underbrace{\bar{B}(t_m, t_{m+1})}_{\text{non-stationarity regret}(\mathfrak{R}_m^{env})} \Bigg).$$

In Theorem 5.3, we articulate the decomposition of $\mathfrak{R}_m(T)$ into three terms: the policy optimization regret, denoted as $\mathfrak{R}_m^{\pi}$, Q value forecasting regret, denoted as $\mathfrak{R}_m^f$, and non-stationarity regret, denoted by $\mathfrak{R}_m^{\text{env}}$. Now, by extending the upper bound of the forecasting error regret to $\sum_{m=1}^{M} \mathfrak{R}_m^f \leq \sum_{m=1}^{M} (N_m + G_m)(C_2\delta_f + C_3) = T(C_2\delta_f + C_3) \leq T\left(C_2 \left(Lu_{\max}\sqrt{2l_p} + l_p(L+1)\left(\frac{1-\gamma^H}{1-\gamma} r_{\max}\right)\right) + C_3\right)$, we find that its upper bound is independent from $\{N_i, G_i\}_{i=1}^{m}$, and satisfies a sublinear convergence rate to the total time T for any $l_p = (1/T)^{\alpha}, \alpha > 0$.

Expanding on the independence of $\{N_i, G_i\}_{i=1}^{m}$ from the upper bound of $\sum_{m=1}^{M} \mathfrak{R}_m^f$, we will show how N_m balances between $\mathfrak{R}_m^{\pi}$ and $\mathfrak{R}_m^{env}$, followed by minimizing the upper bound of $\mathfrak{R}_m(T)$ in the next subsection.

5.2. Theoretical insight

One crucial theoretical insight to be deduced from Theorem 5.3 is which nonzero value of N_m strikes a balance between $\mathfrak{R}_m^{\pi}$ and $\mathfrak{R}_m^{env}$. Our insights begin with the analysis of $\mathfrak{R}_m(T)$. We start by considering a fixed time interval $[t_m, t_{m+1}]$, which brings up the constraint $N_m + G_m = t_{m+1} - t_m$. The initial aspect of our investigation addresses whether a nonzero value of N_m offers any advantage in a *stationary* environment.

Lemma 5.4 (Optimal N_m^*, G_m^* for $\mathfrak{R}_m^{\pi}$)**.** *Given fixed time interval $[t_m, t_{m+1}]$, the optimal values N_m^* and G_m^* that minimize $\mathfrak{R}_m^{\pi}$ are determined as $N_m^* = 0$ and $G_m^* = t_{m+1} - t_m$, respectively.*

Since $\mathfrak{R}_m^{env} = 0$ is satisfied in stationary environments (see Definition 3.3), Corollary 5.5 ensues from Lemma 5.4.

Corollary 5.5 (Optimal N_m^*, G_m^* in Stationary Environments)**.** *Consider a stationary environment. The upper bound of the $\mathfrak{R}_m$ is achieved at its minimum when $N_m = 0$ and $G_m = t_{m+1} - t_m$, respectively.*

What Corollary 5.5 states is intuitively straightforward. This is because in scenarios where the time sequence of the policy update $(t_1, t_2, \ldots, t_m)$ is fixed, maximizing the policy update duration is advantageous without considering forecasting errors. However, we claim that N_m plays an important role in a non-stationary environment, i.e., positive N_m^* minimizes the upper bound of $\mathfrak{R}_m(T)$. We first develop the following proposition.

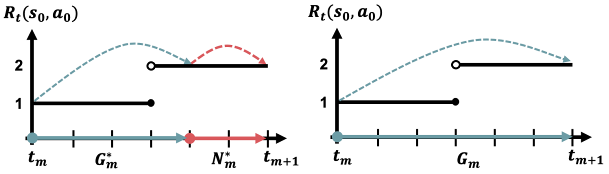

(a) (b)

Figure 3. Optimal solutions for $\min_{G_m, N_m} \bar{B}(t_m, t_{m+1})$ are $(G_m^*, N_m^*) = (4, 2), (2, 4)$ (a) $G_m = 4, N_m = 2$ (b) $G_m = 6, N_m = 0$

Proposition 5.6 (Existence of Positive N_m^* for $\mathfrak{R}_m^{\text{env}}$)**.** *In a non-stationary environment, consider any given time interval $[t_m, t_{m+1}]$ satisfying $t_{m+1} - t_m \geq 2$. Under these conditions, there exists a number N_m within the open interval $(0, t_{m+1} - t_m)$ that minimizes $\bar{B}(t_m, t_{m+1})$.*

One way to intuitively understand Proposition 5.6 is exemplified in Figure 3. Consider a non-stationary environment where the reward abruptly changes only at state s_0 and action a_0. Suppose that $C_4 = C_5 = 1$. Then $\min \bar{B}(t_m, t_{m+1}) = 1$ and its solution is attainable at $(G_m^*, N_m^*) = (4, 2)$ and $(2, 4)$ (Figure 3 (a)), while in the case where $G_m = 6, N_m = 0$ yields $\bar{B}(t_m, t_{m+1}) = 3$ (Figure 3 (b)). Both subfigures optimize the policy toward the forecasted future Q value of time t_{m+1}, but the time that the agent stops to update the policy ($t = t_m + G_m$) determines how much the agent would be conservative with respect to the future reward prediction.

Based on Proposition 5.6, we introduce the surrogate optimal solution (G_m^*, N_m^*) for the non-stationarity regret $\mathfrak{R}_m^{env}$. According to Corollary 3.2, it holds that $\bar{B}_r(\mathcal{N}_m)$ is bounded by $\sum_{t=t_m+G_m}^{t=t_m+G_m+N_m-1} \alpha_r^{t-(t_m+G_m)} B_r^{\max}(\mathcal{N}_m)$, and similarly, $\bar{B}_r(\mathcal{G}_m)$ is bounded by $\sum_{t=t_m}^{t=t_m+G_m-1} \alpha_r^{t-t_m} B_r^{\max}(\mathcal{G}_m)$. For brevity, we use the notation $\alpha_{\diamond,1} = \alpha_{\diamond}(\mathcal{G}_m)$ and $\alpha_{\diamond,2} = \alpha_{\diamond}(\mathcal{N}_m)$, and similarly for $B_{\diamond,1}^{\max} = B_{\diamond}^{\max}(\mathcal{G}_m)$ and $B_{\diamond,2}^{\max} = B_{\diamond}^{\max}(\mathcal{N}_m)$, where $\diamond$ is either r or p. Furthermore, we define $\alpha_{\square}$ as the $\max\left(\alpha_{r,\square}, \alpha_{p,\square}\right)$, and $B_{\square}^{\max}$ as the $\max\left(B_{r,\square}^{\max}, B_{p,\square}^{\max}\right)$, where $\square$ is either 1 or 2.

Lemma 5.7 (Surrogate optimal (G_m^*, N_m^*) for $\mathfrak{R}_m^{env}$)**.** *For given m, t_m, t_{m+1}, the surrogate optimal policy update and policy hold variables that minimize the upper bound of $\mathfrak{R}_m^{env}$ are*

$$N_m^* = \underset{N_m \in \{\lfloor \tilde{N}_m^* \rfloor, \lfloor \tilde{N}_m^* \rfloor + 1\}}{\arg\min} \mathfrak{R}_m^{env}(N_m, G_m)$$

and

$$G_m^* = t_{m+1} - t_m - N_m^*,$$

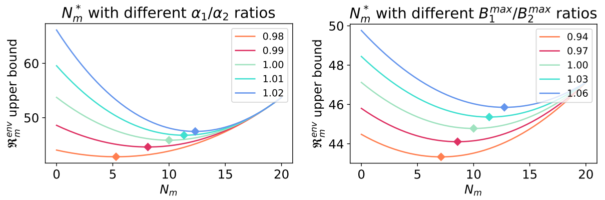

(a) (b)

Figure 4. $\mathfrak{R}_m^{\text{env}}$ upper bound with different environmental hyperparameters. ♦ denotes the minimum of each function graph. (a) $\alpha_1/\alpha_2 \in \{0.98, 0.99, 1.0, 1.01, 1.02\}$. (b) $B_1^{\max}/B_2^{\max} \in \{0.94, 0.97, 1.0, 1.03, 1.06\}$.

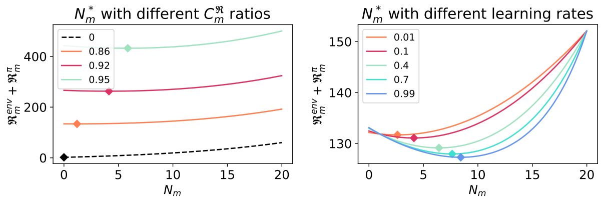

(a) (b)

Figure 5. $\mathfrak{R}_m^{\text{env}} + \mathfrak{R}_m^{\pi}$ upper bound with different $C_{\mathfrak{R}}$ ratios and learning rates. ♦ denotes the minimum of each function graph. (a) $C_m^{\mathfrak{R}} \in \{0, 0.86, 0.92, 0.95\}$. (b) Learning rates $\in \{0.01, 0.1, 0.3, 0.7, 0.99\}$.

where

$$\tilde{N}_m^* = \frac{1}{\ln(\alpha_2/\alpha_1)} \cdot \ln\left(\frac{\ln\alpha_1/(\alpha_1-1)}{\ln\alpha_2/(\alpha_2-1)} \cdot \alpha_1^{t_{m+1}-t_m} \cdot \frac{B_1^{max}}{B_2^{max}}\right).$$

Note that Lemma 5.7 provides a nonzero suboptimal N_m^* that minimizes the non-stationary regret $\mathfrak{R}_m^{env}$. Now, we combine Lemmas 5.4 and 5.7 to find the suboptimal N_m^* and G_m^* that minimize the upper bound of $\mathfrak{R}_m(T)$.

Theorem 5.8 (Surrogate optimal (G_m^*, N_m^*) for $\mathfrak{R}_m$)**.** *For given m, t_m, t_{m+1}, the surrogate optimal policy update variable N_m and surrogate policy hold variable G_m that minimize the upper bound of $\mathfrak{R}_m$ satisfy the following equation:*

$$C_1\left((N_m-1)\ln(1-\eta\tau)-1\right)(1-\eta\tau)^{G_m} +$$
$$(C_4+C_5)\left(\frac{\ln\alpha_1}{\alpha_1-1}B_1^{max}\alpha_1^{G_m} - \frac{\ln\alpha_2}{\alpha_2-1}B_2^{max}\alpha_2^{N_m}\right) = 0,$$

where $C_1, C_4, C_5, \eta, \tau, \alpha_1, \alpha_2, B_1^{max}$, and B_2^{max} are constants or parameters specific to the system under consideration.

Apart from Lemma 5.7, Theorem 5.8 does not provide a closed-form solution. Consequently, we will conduct some numerical experiments to understand how N_m^* and G_m^* change to the hyperparameters of Theorem 5.8 in the next subsection.

5.3. Numerical analysis of theoretical insights

Figures 4 and 5 show how the surrogate optimal N_m^* changes with different parameter choices. Figure 4 shows how N_m^* changes with different parameters of the environment intrinsic uncertainty. Note that $(\alpha_1, B_1^{\max})$ and $(\alpha_2, B_2^{\max})$ represent the magnitude (severity) of the intrinsic uncertainty of the environment during the policy update phase ($\mathcal{G}_m$) and the policy hold phase ($\mathcal{N}_m$), respectively. The two subfigures of Figure 4 not only support the importance of holding N_m^*, but also show the necessity of keeping the policy hold phase longer if the uncertainty of the environment during the policy update phase $(\alpha_1, B_1^{\max})$ is greater than that of the policy hold phase $(\alpha_2, B_2^{\max})$. Moreover, Figure 5 (a) shows that increasing N_m^* provides a better performance if the environment regret term dominates the regret $\mathfrak{R}_m^{\text{env}} + \mathfrak{R}_m^{\pi}$. We define the dominant ratio $C_m^{\mathfrak{R}}$ as $C_m^{\mathfrak{R}} := \int_{t_m}^{t_{m+1}} \mathfrak{R}_m^{env}/(\mathfrak{R}_m^{env} + \mathfrak{R}_m^{\pi})dt$. Finally, Figure 5 (b) validates that the surrogate optimal solution is still an acceptable solution and illustrates that the suboptimal gap resulting from relaxing the non-convex upper bound into a convex one is tolerable, as a higher learning rate leads to a fast convergence of $\mathfrak{R}_m^{\pi}$ and, in turn, intuitively results in a longer N_m within fixed t_m, t_{m+1}.

6. Experiments

In this section, we demonstrate the effectiveness of two key components of the proposed algorithm, forecasting Q value (line 7 of Algorithm 1) and the strategic policy update (line 9 $\sim$ 12 of Algorithm 1). In Subsection 6.2, we illustrate how utilizing forecasted Q value yields higher rewards compared to a reactive method in a finite-dimensional environment. Subsequently, in Subsection 6.3, we will show how strategically assigning different policy update frequencies provides a higher performance than the continually updating policy method in an infinite-dimensional Mujoco environment, swimmer and halfcheetah. Details of environments and experiments are specified in Appendix B.

6.1. Future Q value estimator

For the following experiments in Subsections 6.2 and 6.3, we design the `ForQ` function as the least-squares estimator (Chandak et al., 2020b), namely $\tilde{Q}_{t_{m+1}|t_m}(s,a) = \phi(t_{m+1})^\top w^*(s,a)$ where $\phi : [0,T) \to \mathbb{R}^d$ is a basis function for encoding the time index. For example, an identity basis is $\phi(x) := \{x, 1\}$. Then $w^*(s,a)$ denotes an optimal solution of the least-squares problem for any $s \in \mathcal{S}, a \in \mathcal{A}$, namely $w^*(s,a) = \arg\min_{w \in \mathbb{R}^{d\times 1}} ||\boldsymbol{Q}(s,a) - \Phi(X)^\top w||_2$ where $\boldsymbol{Q}(s,a) := [Q_{t_m - l_p + 1}(s,a), \ldots, Q_{t_m}(s,a)]^\top \in \mathbb{R}^{l_p \times 1}$, $X := [t_m - l_p + 1, \ldots, t_m]^\top \in \mathbb{R}^{l_p \times 1}$, and $\Phi(X) := [\phi(t_m - l_p + 1), \ldots, \phi(t_m)] \in \mathbb{R}^{d \times l_p}$. The solution to the above least-squares problem is $w^*(s,a) =$

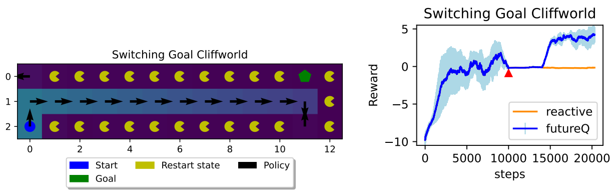

(a) (b)

Figure 6. (a) Swithcing goal cliffworld. (b) Reward per step. A red triangle means the goal point switches at step $= 10000$. A shaded area denotes one standard deviation among five different hyperparameter results.

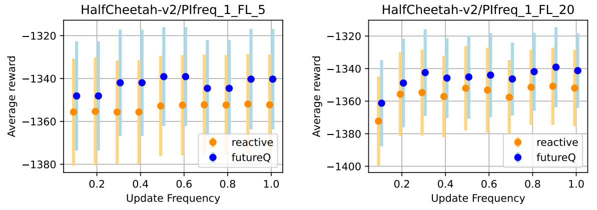

(a) (b)

Figure 7. Halfcheetah environment: blue dots are FSAC and orange dots are SAC. An error bar is 0.5 standard deviation over 36 different hyperparmeter results. (a) Average reward $l_f = 5$. (b) Average reward $l_f = 20$.

$(\Phi(X)^\top \Phi(X))^{-1} \Phi(X)^\top \boldsymbol{Q}(s, a)$.

6.2. Goal switching cliffworld

We first experiment with a low-dimensional tabular MDP to verify that evaluating the policy by the forecasting method yields a better performance than the reactive method. The environment is the switching goal cliffworld where the agent always starts in the blue circle and a goal switches between two green pentagons (Figure 6 (a)). We use the Q-learning algorithm (Watkins & Dayan, 1992) to evaluate the current policy and compute future policy with future Q estimator proposed in Subsection 6.1. Figure 6 (b) illustrates that after the goal point switches at step $= 10000$, the reactive method fails to obtain an optimal policy for the remaining steps. In contrast, the forecasting Q method successfully identifies an optimal policy shortly after step $= 15000$.

6.3. Mujoco environment

To verify our findings in a large-scale environment, we propose a practical deep learning algorithm, Forecasting Soft-Actor Critic (FSAC), that specifies Algorithm 1. The FSAC algorithm is detailed in Algorithm 3 (see Appendix A). Then, we conduct experiments in high-dimensional non-stationary Mujoco environments (Todorov et al., 2012), swimmer, and halfcheetah where the reward changes as the episode goes by (Feng et al., 2022). We utilize the Soft-Actor Critic (SAC) algorithm (Haarnoja et al., 2018) as a baseline.

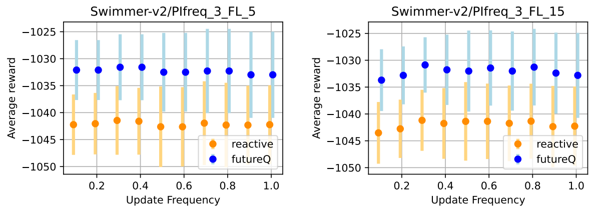

(a) (b)

Figure 8. Swimmer environment: blue dots are FSAC and orange dots are SAC. An error bar is 0.5 standard deviation over 36 different hyperparmeter results. (a) Average reward $l_f = 5$. (b) Average reward $l_f = 15$.

In particular, the distinctions between the FSAC and the SAC are the lines 2, $9 \sim 11$, and $16 \sim 18$ of Algorithm 3. In FSAC, the prediction length $l_f \in \mathbb{N}$ and the update frequency $\gamma_f \in (0, 1]$ are set as hyperparameters, with $t_m = l_f m$ for all $m \in [M]$ (line 2). The algorithm forecasts future Q values at every l_f iteration (lines $9 \sim 11$), updating the policy during the interval $(t_m, t_m + \lfloor l_f \gamma_f \rfloor]$ and keeping it between $(t_m + \lfloor l_f \gamma_f \rfloor, t_{m+1}]$ (lines $16 \sim 18$).

Figures 7 and 8 depict the results. In most cases, the FSAC algorithm (indicated by blue dots) yields a higher average return compared to the SAC algorithm (indicated by orange dots). These practical experiments aim to emphasize that $\gamma_f = 1.0$ does not necessarily lead to the best average reward. This observation aligns with our theoretical analysis presented in Section 5.2, where we demonstrate that a non-negative N_m^* minimizes the upper bound of dynamic regret. We will elaborate on training and result details in Appendix B.2.

7. Conclusion

This paper introduces a forecasting online reinforcement learning framework, demonstrating that non-zero policy hold durations improve dynamic regret's upper bound. Empirical results show the forecasting method's advantage over reactive approaches and indicate that continuous policy updates do not always maximize average rewards. For future work, it is crucial to explore methods to minimize the forecasting error to achieve a sharper upper bound. This paper presents work whose goal is implementing real-time control with prediction in environments with unknown uncertainties. A significant societal impact of our research is the narrowing of the gap between simulation-based RL and its real-world applications, along with demonstrating the advantages of pausing model learning in continual learning settings.

References

Adam, S., Busoniu, L., and Babuska, R. Experience replay for real-time reinforcement learning control. *IEEE Transactions on Systems, Man, and Cybernetics, Part C (Applications and Reviews)*, 42(2):201–212, 2012.

Cai, H., Ren, K., Zhang, W., Malialis, K., Wang, J., Yu, Y., and Guo, D. Real-time bidding by reinforcement learning in display advertising. In *Proceedings of the tenth ACM international conference on web search and data mining*, pp. 661–670, 2017.

Cen, S., Cheng, C., Chen, Y., Wei, Y., and Chi, Y. Fast global convergence of natural policy gradient methods with entropy regularization. *Operations Research*, 70(4): 2563–2578, 2022.

Chandak, Y., Jordan, S., Theocharous, G., White, M., and Thomas, P. S. Towards safe policy improvement for non-stationary mdps. *Advances in Neural Information Processing Systems*, 33:9156–9168, 2020a.

Chandak, Y., Theocharous, G., Shankar, S., White, M., Mahadevan, S., and Thomas, P. Optimizing for the future in non-stationary mdps. In *International Conference on Machine Learning*, pp. 1414–1425. PMLR, 2020b.

Covington, P., Adams, J., and Sargin, E. Deep neural networks for youtube recommendations. In *Proceedings of the 10th ACM Conference on Recommender Systems*, 2016.

Dulac-Arnold, G., Mankowitz, D., and Hester, T. Challenges of real-world reinforcement learning. *arXiv preprint arXiv:1904.12901*, 2019.

Espeholt, L., Soyer, H., Munos, R., Simonyan, K., Mnih, V., Ward, T., Doron, Y., Firoiu, V., Harley, T., Dunning, I., et al. Impala: Scalable distributed deep-rl with importance weighted actor-learner architectures. In *International conference on machine learning*, pp. 1407–1416. PMLR, 2018.

Evans, R. and Gao, J. Deepmind ai reduces google data centre cooling bill by 40 URL https://deepmind.google/discover/blog/.

Even-Dar, E. and Mansour, Y. Learning rates for q-learning. *J. Mach. Learn. Res.*, 5:1–25, dec 2004. ISSN 1532-4435.

Feng, F., Huang, B., Zhang, K., and Magliacane, S. Factored adaptation for non-stationary reinforcement learning. *Advances in Neural Information Processing Systems*, 35: 31957–31971, 2022.

Finn, C., Rajeswaran, A., Kakade, S., and Levine, S. Online meta-learning. In *International Conference on Machine Learning*, pp. 1920–1930. PMLR, 2019.

Gal, Y. Uncertainty in deep learning. phd thesis, University of Cambridge, 2016.

Glavic, M., Fonteneau, R., and Ernst, D. Reinforcement learning for electric power system decision and control: Past considerations and perspectives. *International Federation of Automatic Control*, 50:6918–6927, 2017.

Haarnoja, T., Zhou, A., Abbeel, P., and Levine, S. Soft actor-critic: Off-policy maximum entropy deep reinforcement learning with a stochastic actor. In *International conference on machine learning*, pp. 1861–1870. PMLR, 2018.

Hester, T. and Stone, P. Texplore: real-time sample-efficient reinforcement learning for robots. *Machine learning*, 90: 385–429, 2013.

Imanberdiyev, N., Fu, C., Kayacan, E., and Chen, I.-M. Autonomous navigation of uav by using real-time model-based reinforcement learning. *2016 14th International Conference on Control, Automation, Robotics and Vision (ICARCV)*, 2016.

Kakade, S. M. A natural policy gradient. *Advances in neural information processing systems*, 14, 2001.

Lee, H., Ding, Y., Lee, J., Jin, M., Lavaei, J., and Sojoudi, S. Tempo adaptation in non-stationary reinforcement learning. *arXiv preprint arXiv:2309.14989*, 2023.

Levine, N., Chow, Y., Shu, R., Li, A., Ghavamzadeh, M., and Bui, H. Prediction, consistency, curvature: Representation learning for locally-linear control. *arXiv preprint arXiv:1909.01506*, 2019.

Mao, W., Zhang, K., Zhu, R., Simchi-Levi, D., and Basar, T. Near-optimal model-free reinforcement learning in non-stationary episodic mdps. In *Proceedings of the 38th International Conference on Machine Learning*, volume 139 of *Proceedings of Machine Learning Research*, pp. 7447–7458. PMLR, 2021.

Qu, G. and Wierman, A. Finite-time analysis of asynchronous stochastic approximation and q-learning. In Abernethy, J. and Agarwal, S. (eds.), *Proceedings of Thirty Third Conference on Learning Theory*, volume 125 of *Proceedings of Machine Learning Research*, pp. 3185–3205. PMLR, 09–12 Jul 2020.

Ramstedt, S. and Pal, C. Real-time reinforcement learning. *Advances in neural information processing systems*, 32, 2019.

Schrittwieser, J., Antonoglou, I., Hubert, T., Simonyan, K., Sifre, L., Schmitt, S., Guez, A., Lockhart, E., Hassabis, D., Graepel, T., et al. Mastering atari, go, chess and shogi by planning with a learned model. *Nature*, 588(7839): 604–609, 2020.

Silver, D., Huang, A., Maddison, C. J., Guez, A., Sifre, L., van den Driessche, G., Schrittwieser, J., Antonoglou, I., Panneershelvam, V., Lanctot, M., Dieleman, S., Grewe, D., Nham, J., Kalchbrenner, N., Sutskever, I., Lillicrap, T., Leach, M., Kavukcuoglu, K., Graepel, T., and Hassabis, D. Mastering the game of go with deep neural networks and tree search. *Nature*, 529:484–503, 2016.

Spirtes, P. An anytime algorithm for causal inference. In *Proceedings of the Eighth International Workshop on Artificial Intelligence and Statistics*, volume R3 of *Proceedings of Machine Learning Research*, pp. 278–285. PMLR, 04–07 Jan 2001.

Steck, H., Baltrunas, L., Elahi, E., Liang, D., Raimond, Y., and Basilico, J. Deep learning for recommender systems: A netflix case study. *AI Magazine*, 42(3):7–18, 2021.

Todorov, E., Erez, T., and Tassa, Y. Mujoco: A physics engine for model-based control. In *2012 IEEE/RSJ International Conference on Intelligent Robots and Systems*, pp. 5026–5033. IEEE, 2012.

Vlasselaer, J., Van den Broeck, G., Kimmig, A., Meert, W., and De Raedt, L. Anytime inference in probabilistic logic programs with tp-compilation. In *Proceedings of 24th International Joint Conference on Artificial Intelligence (IJCAI)*, volume 2015, pp. 1852–1858. IJCAI-INT JOINT CONF ARTIF INTELL, 2015.

Wang, J. and Yuan, S. Real-time bidding: A new frontier of computational advertising research. *Proceedings of the Eighth ACM International Conference on Web Search and Data Mining*, 2015.

Watkins, C. J. and Dayan, P. Q-learning. *Machine learning*, 8:279–292, 1992.

A. Algorithms

Algorithm 2 `Update`: Update policy π

```
**Input:** policy $\pi$, learning rate $\eta$, entropy regularization constant $\tau$, discount factor $\gamma$, policy evaluation $\widehat{Q}$
$Z(s) = \sum_{a \in \mathcal{A}} (\pi(a|s))^{1-\frac{\eta\tau}{1-\gamma}} \exp\left(\eta\widehat{Q}(s,a)/(1-\gamma)\right)$
$\pi'(\cdot|s) = \frac{1}{Z(s)} \cdot (\pi(\cdot|s))^{1-\frac{\eta\tau}{1-\gamma}} \exp\left(\frac{\eta\widehat{Q}(s,\cdot)}{1-\gamma}\right)$
**Return** $\pi'$
```

Algorithm 3 Forecasting Soft Actor-Critic

```
Initialize parameter vectors $\psi, \bar{\psi}, \theta, \phi$.
Set prediction length $l_f$, update frequency $\gamma_f$
for each iteration do
    for each environment step do
        Sample action $a_t \sim \pi_\theta(a_t|s_t)$.
        Sample next state $s_{t+1} \sim p(s_{t+1}|s_t, a_t)$.
        $D \leftarrow D \cup \{(s_t, a_t, r(s_t, a_t), s_{t+1})\}$.
    end for
    if iteration $\%\ l_f = 0$ then
        $\tilde{Q} = \texttt{ForQ}(D)$.
    end if
    for each gradient step do
        $\psi \leftarrow \psi - \lambda_\psi \nabla_\psi J_V(\psi)$.
        $\theta_i \leftarrow \theta_i - \lambda_Q \nabla_{\theta_i} J_Q(\theta_i)$ for $i \in \{1, 2\}$.
        $\bar{\psi} \leftarrow \tau_s \psi + (1 - \tau_s)\bar{\psi}$.
        if iteration $\%\ l_f \leq l_f \gamma_f$ then
            $\phi \leftarrow \phi - \lambda_\pi \nabla_\phi \tilde{J}_\pi(\phi)$.
        end if
    end for
end for
```

B. Experiments

B.1. Environments and experiments details

Goal switching cliffword

The environment is 12×3 tabular MDP where $(0, 2)$ is a fixed initial state (blue point), and the possible goal points are $(11, 0)$ and $(11, 2)$ (for the x, y axis, see Figure 6 (a)). The agent executes 4 actions (up, left, right, down). If the agent reaches the restart states ($(1, 2), (2, 2), ..., (10, 2)$ and $(1, 0), (2, 0), ..., (10, 0)$), denoted by yellow points, then the agent goes back to the initial state with a failure reward -100. If the agent reaches the goal point, then it receives the success reward $+100$. For taking every step (for every time the agent executes an action), the agent receives a step reward of -100.

For experiments, we use the Q-learning algorithm (Watkins & Dayan, 1992). In Figure 6 (b), we denote “reactive” label as Q-learning algorithm proposed by (Watkins & Dayan, 1992) and “future Q” label as a method that combines Q-learning algorithm to evaluate the current policy and use future Q estimator to compute future policy that was proposed in section 6.1. We set the maximum number of steps as 100. The experiments have been carried out by changing hyperparameters of Q-learning: step size α and ϵ from the ϵ-greedy method. We have done experiments with different $(\alpha, \epsilon) = (0.05, 0.05), (0.1, 0.1), (0.1, 0.05), (0.2, 0.1), (0.2, 0.05), (0.3, 0.1)$.

Swimmer, Halfcheetah

The Swimmer and Halfcheetah environments share the same reward function at step h as $r_h = r_h^{(1)} + r_h^{(2)} + r_h^{(3)}$. It comprises a healthy reward ($r_h^{(1)}$), a forward reward ($r_h^{(2)} = k_f \frac{x_{h+1} - x_h}{\Delta t_{frame}}, k_f > 0$), and a control cost ($r_h^{(3)}$). We modify the environment to be non-stationary by the agent's desired velocity changes as time goes by. Specifically, we modify the forward reward $r_h^{(2)}$ varies as $r_h^{(2)} = -\left|k_f \frac{x_{h+1}-x_h}{\Delta t_{frame}} - v_d(t)\right|$, with $v_d(t) = a\sin(wt)$ and t representing the episode. Here, $a, w > 0$ are constants.

For our experiments, we varied hyperparameters such as learning rates $\lambda_\pi \in \{0.0001, 0.0003, 0.0005, 0.0007\}$, soft update parameters $\tau_s \in \{0.001, 0.005, 0.003\}$ and the entropy regularization parameters $\{0.01, 0.03, 0.1\}$ and also experimented with different prediction lengths $l_f \in \{5, 15, 20\}$. We selected the average reward per episode as the performance metric, in line with the definition of dynamic regret. For given hyperparameters, we compare the average reward between FSAC and SAC for different update frequencies $\gamma_f \in \{0.1, 0.2, \ldots, 1.0\}$. The experiments were conducted in two different Mujoco environments: HalfCheetah and Swimmer (see Figures 7 and 8). In Figures 7 and 8, error bars denote 0.5 standard deviations.

B.2. Results

In this subsection, we have elaborated detailed results of the experiment on Halfcheetah and Swimmer. Note that Figures 9,11 and 12 are detailed results for Figure 7 of the main paper, and Figures 10,13 and 14 are detailed result for Figure 8 of the main paper. Figures 9 and 10 show the reward return per episode for different update frequencies $\gamma_f \in \{0.1, 0.2, 0.3, 0.4, 0.5, 0.6, 0.7, 0.8, 0.9, 1.0\}$. Figures 11,12,13 and 14 compare the FSAC and SAC reward return per episode. Note that the plotted lines are mean rewards calculated over 36 different hyperparameters (learning rates $\lambda_\pi \in \{0.0001, 0.0003, 0.0005, 0.0007\}$, soft update parameters $\tau_s \in \{0.001, 0.005, 0.003\}$ and the entropy regularization parameters $\{0.01, 0.03, 0.1\}$).

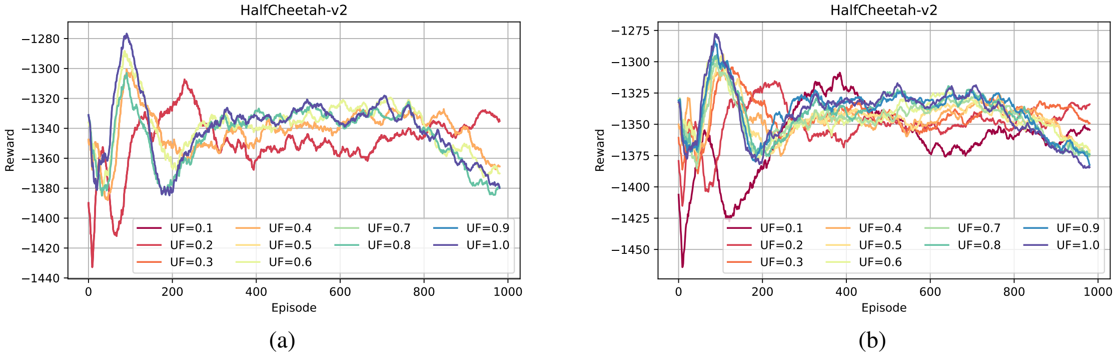

(a)

(b)

Figure 9. Reward per episode in the Halfcheetah environment for various update frequencies $\gamma_f \in \{0.1, 0.2, 0.3, 0.4, 0.5, 0.6, 0.7, 0.8, 0.9, 1.0\}$. The plotted lines represent the mean reward across 36 different hyperparameters. (a) For $l_f = 5$. (b) For $l_f = 20$.

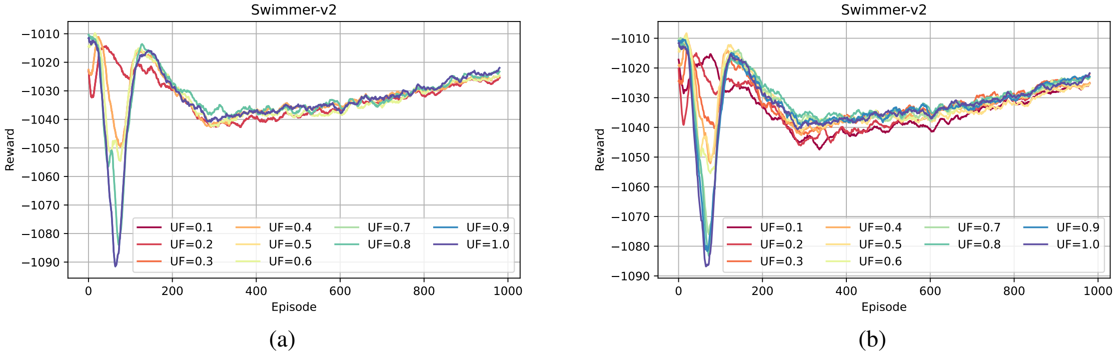

(a)

(b)

Figure 10. Reward per episode in the Swimmer environment for various update frequencies $\gamma_f \in \{0.1, 0.2, 0.3, 0.4, 0.5, 0.6, 0.7, 0.8, 0.9, 1.0\}$. The plotted lines represent the mean reward across 36 different hyperparameters. (a) For $l_f = 5$. (b) For $l_f = 15$.

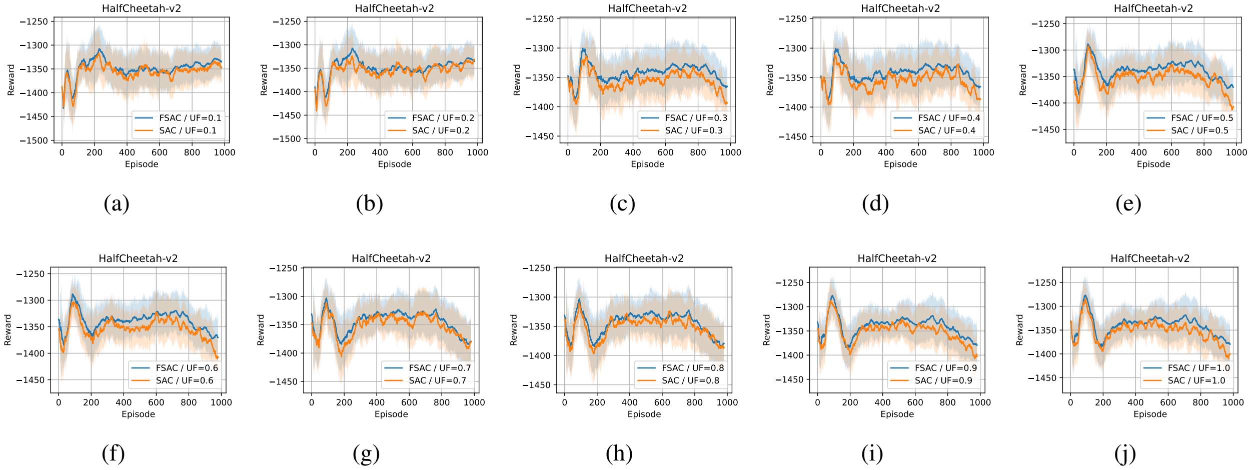

(a) (b) (c) (d) (e)

(f) (g) (h) (i) (j)

Figure 11. Reward per episode for Halfcheetah environment when $l_f = 5$. The blue lines are FSAC, and the orange lines are SAC. The shaded areas are 0.5 standard deviations over 36 different hyperparameter results. (a) $\gamma_f = 0.1$. (b) $\gamma_f = 0.2$. (c) $\gamma_f = 0.3$. (d) $\gamma_f = 0.4$. (e) $\gamma_f = 0.5$. (f) $\gamma_f = 0.6$. (g) $\gamma_f = 0.7$. (h) $\gamma_f = 0.8$. (i) $\gamma_f = 0.9$. (j) $\gamma_f = 1.0$.

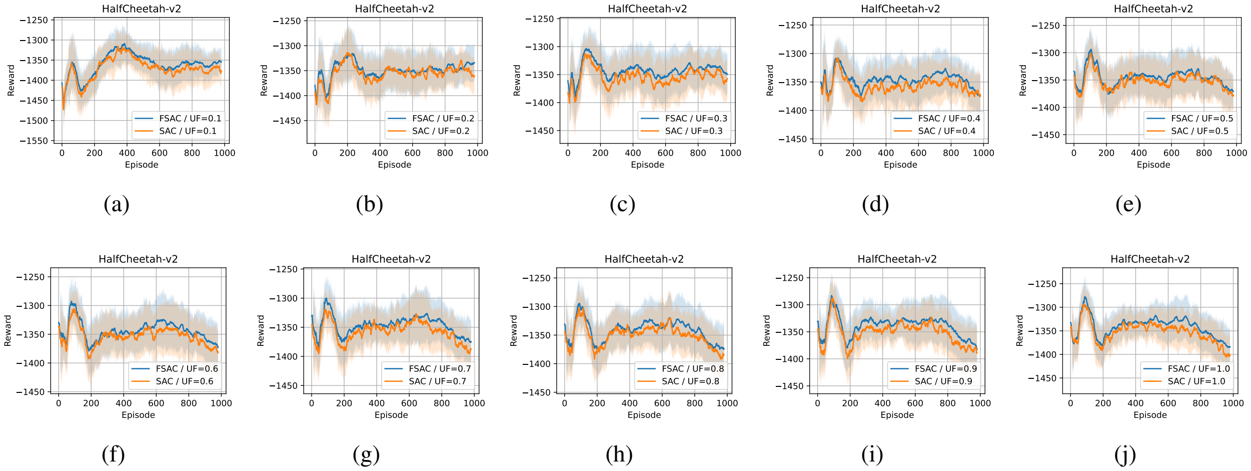

(a) (b) (c) (d) (e)

(f) (g) (h) (i) (j)

Figure 12. Reward per episode for Halfcheetah environment when $l_f = 20$. The blue lines are FSAC, and the orange lines are SAC. The shaded areas are 0.5 standard deviations over 36 different hyperparameter results. (a) $\gamma_f = 0.1$. (b) $\gamma_f = 0.2$. (c) $\gamma_f = 0.3$. (d) $\gamma_f = 0.4$. (e) $\gamma_f = 0.5$. (f) $\gamma_f = 0.6$. (g) $\gamma_f = 0.7$. (h) $\gamma_f = 0.8$. (i) $\gamma_f = 0.9$. (j) $\gamma_f = 1.0$.

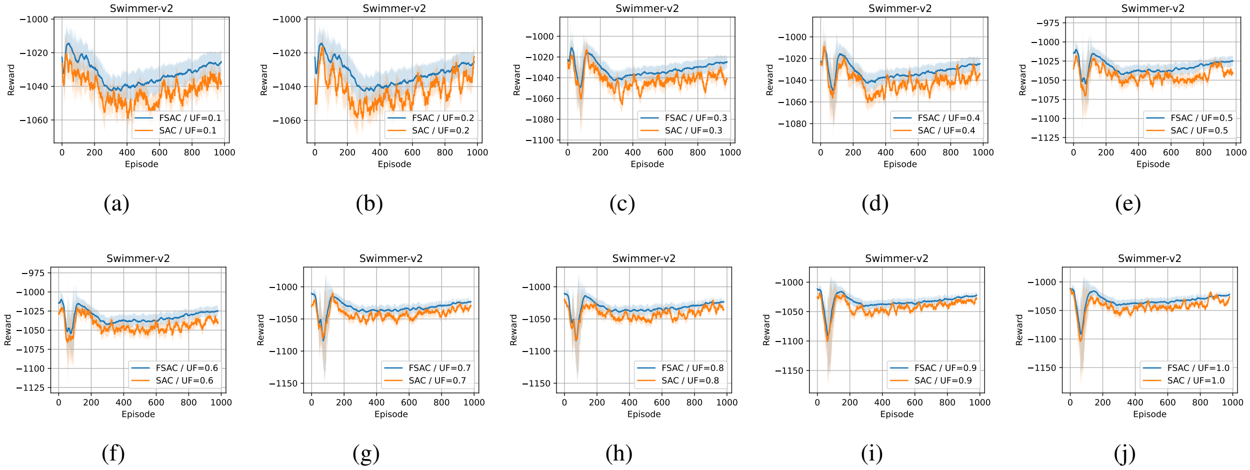

(a) (b) (c) (d) (e)

(f) (g) (h) (i) (j)

Figure 13. Reward per episode for Swimmer environment when $l_f = 5$. The blue lines are FSAC, and the orange lines are SAC. The shaded areas are 0.5 standard deviations over 36 different hyperparameter results. (a) $\gamma_f = 0.1$ (b) $\gamma_f = 0.2$ (c) $\gamma_f = 0.3$ (d) $\gamma_f = 0.4$ (e) $\gamma_f = 0.5$ (f) $\gamma_f = 0.6$ (g) $\gamma_f = 0.7$ (h) $\gamma_f = 0.8$ (i) $\gamma_f = 0.9$ (j) $\gamma_f = 1.0$

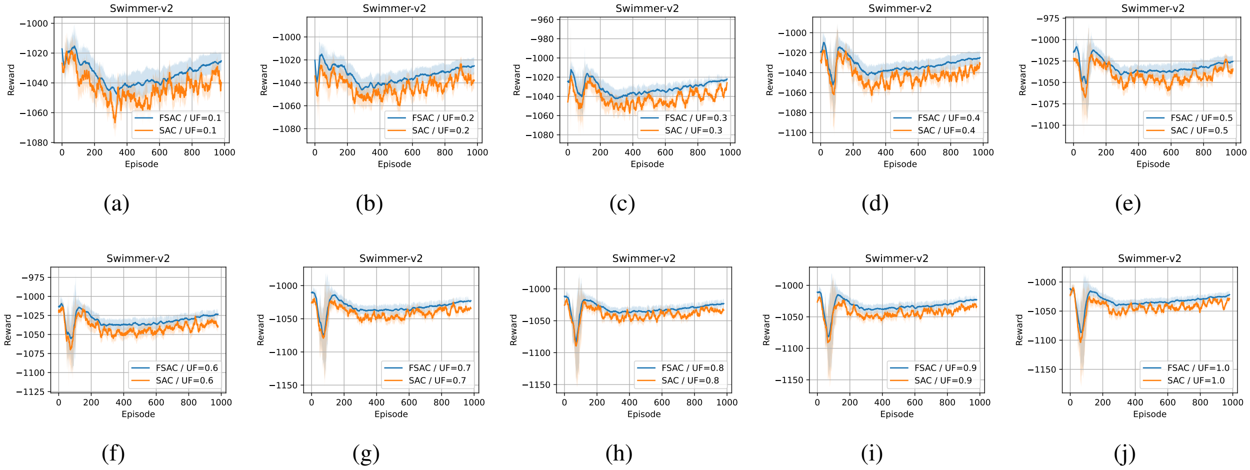

(a) (b) (c) (d) (e)

(f) (g) (h) (i) (j)

Figure 14. Reward per episode for Swimmer environment when $l_f = 15$. The blue lines are FSAC, and the orange lines are SAC. The shaded areas are 0.5 standard deviations over 36 different hyperparameter results. (a) $\gamma_f = 0.1$ (b) $\gamma_f = 0.2$ (c) $\gamma_f = 0.3$ (d) $\gamma_f = 0.4$ (e) $\gamma_f = 0.5$ (f) $\gamma_f = 0.6$ (g) $\gamma_f = 0.7$ (h) $\gamma_f = 0.8$ (i) $\gamma_f = 0.9$ (j) $\gamma_f = 1.0$

C. Proofs

Proof of Proposition 4.1.

$$\begin{aligned}
||\widetilde{Q}_{t_{m+1}} - Q^*_{t_{m+1}}||_\infty &= \left|\left| \sum_{t=t_m-l_p+1}^{t_m} w_t \left(\widehat{Q}_t - Q^*_{t_{m+1}}\right) \right|\right|_\infty + \left|\left| \sum_{t=t_m-l_p+1}^{t_m} (w_t - 1)\, Q^*_{t_{m+1}} \right|\right|_\infty \\
&\leq \sum_{t=t_m-l_p+1}^{t_m} |w_t| \left(||Q^*_t - Q^*_{t_{m+1}}||_\infty + ||Q^*_t - \widehat{Q}_t||_\infty \right) + \sum_{t=t_m-l_p+1}^{t_m} |w_t - 1| \left|\left| Q^*_{t_{m+1}} \right|\right|_\infty \\
&\leq \sqrt{\sum_{t=t_m-l_p+1}^{t_m} |w_t|^2} \sqrt{\sum_{t=t_m-l_p+1}^{t_m} \left(||Q^*_t - Q^*_{t_{m+1}}||_\infty + ||Q^*_t - \widehat{Q}_t||_\infty \right)^2} \\
&\quad + \left(\sum_{t=t_m-l_p+1}^{t_m} |w_t| + l_p \right) \left|\left| Q^*_{t_{m+1}} \right|\right|_\infty \\
&\leq L \cdot \sqrt{\sum_{t=t_m-l_p+1}^{t_m} \left(||Q^*_t - Q^*_{t_{m+1}}||^2_\infty + 2||Q^*_t - Q^*_{t_{m+1}}||_\infty ||Q^*_t - \widehat{Q}_t||_\infty ||Q^*_t - \widehat{Q}_t||^2_\infty \right)} \\
&\quad + \left(l_p \sqrt{\sum_{t=t_m-l+1}^{t_m} |w_t|^2} + l_p \right) \left(\frac{1-\gamma^H}{1-\gamma} r_{max} \right) \qquad (1)
\end{aligned}$$

We use the lemma D.2 that

$$||Q^*_t - Q^*_{t_{m+1}}||_\infty \leq \frac{1-\gamma^H}{1-\gamma} \left(B_r(t, t_{m+1}) + \frac{r_{max}}{1-\gamma} B_p(t, t_{m+1}) \right)$$

holds and the assumption

$$||Q^*_t - \widehat{Q}_t||_\infty \leq \epsilon_t$$

holds. Then, we finally have the following.

$$\begin{aligned}
&\left|\left| \widetilde{Q}_{t_{m+1}} - Q^*_{t_{m+1}} \right|\right|_\infty \\
&\leq L \sqrt{\sum_{t=t_m-l+1}^{t_m} \left[\left(\frac{1-\gamma^H}{1-\gamma} \left(B_r(t, t_{m+1}) + \frac{r_{max}}{1-\gamma} B_p(t, t_{m+1}) \right) \right)^2 + 2\frac{1-\gamma^H}{1-\gamma} \left(B_r(t, t_{m+1}) + \frac{r_{max}}{1-\gamma} B_p(t, t_{m+1}) \right) \epsilon_t + \epsilon_t^2 \right]} \\
&+ \quad l_p(L+1) \left(\frac{1-\gamma^H}{1-\gamma} r_{max} \right)
\end{aligned}$$

or in a simple expression, we let $u_t := \frac{1-\gamma^H}{1-\gamma} \left(B_r(t, t_{m+1}) + \frac{r_{max}}{1-\gamma} B_p(t, t_{m+1}) \right)$. Then inequality 1 can be rewritten in a simpler form as follows.

$$\begin{aligned}
\left|\left| \widetilde{Q}_{t_{m+1}} - Q^*_{t_{m+1}} \right|\right|_\infty &\leq L \sqrt{\sum_{t=t_m-l+1}^{t_m} 2\left(\max(u_t, \epsilon_t)\right)^2} + l_p(L+1) \left(\frac{1-\gamma^H}{1-\gamma} r_{max} \right) \\
&\leq \sqrt{2} L l_p \max_{t \in [t_m-l+1, t_m]} \left(\max(u_t, \epsilon_t)\right) + l_p(L+1) \left(\frac{1-\gamma^H}{1-\gamma} r_{max} \right)
\end{aligned}$$

Proof of Proposition 4.2. Refer to Theorem 7 of (Qu & Wierman, 2020). □

□

Proof of Lemma 5.1. The policy update term is divided into three terms.

$$\begin{aligned}\sum_{t\in\mathcal{G}_m}\left(V_t^* - V_t^{\pi_t}\right) &= \sum_{g=0}^{G_m-1}\left(V_{t_m+g}^* - V_{t_m+g}^{\pi_{t_m+g}}\right)\\ &= \sum_{g=0}^{G_m-1}\left(\underbrace{\left(V_{t_m+G_m-1}^* - V_{t_m+G_m-1}^{\pi_{t_m+g}}\right)}_{\text{(1-I)}} + \underbrace{\left(V_{t_m+G_m-1}^{\pi_{t_m+g}} - V_{t_m+g}^{\pi_{t_m+g}}\right)}_{\text{(1-II)}} + \underbrace{\left(V_{t_m+g}^* - V_{t_m+G_m-1}^*\right)}_{\text{(1-III)}}\right)\end{aligned}$$

Note that the term (1-I), the term (1-II), and the term (1-III) are upper bounded by the Lemma D.1, Corollary D.3, and Lemma D.4.

For any $g \in [0, G_m - 1]$ and for any $s \in \mathcal{S}$,

- $V_{t_m+G_m-1}^* - V_{t_m+G_m-1}^{\pi_{t_m+g}} \leq (\gamma+2)((1-\eta\tau)^g C') + \frac{2(\gamma+2)}{1-\gamma}\left(1+\frac{\gamma}{\eta\tau}\right)\cdot\epsilon_f + \frac{2\tau\log|\mathcal{A}|}{1-\gamma}$
- $V_{t_m+G_m-1}^{\pi_{t_m+g}}(s) - V_{t_m+g}^{\pi_{t_m+g}}(s) \leq \frac{1-\gamma^H}{1-\gamma}\cdot B_r(t_m+g, t_m+G_m-1) + \frac{\gamma}{1-\gamma}\cdot\left(\frac{1-\gamma^H}{1-\gamma} - \gamma^{H-1}H\right)\cdot B_p(t_m+g, t_m+G_m-1)$
- $V_{t_m+g}^*(s) - V_{t_m+G_m-1}^*(s) \leq \frac{1-\gamma^H}{1-\gamma}\left(B_r(t_m+g, t_m+G_m-1) + \frac{r_{max}}{1-\gamma}B_p(t_m+g, t_m+G_m-1)\right)$

holds where $C' = ||Q_\tau^* - Q_\tau^{t_m}||_\infty + 2\tau(1-\frac{\eta\tau}{1-\gamma}||\log\pi_\tau^* - \log\pi_\tau^{t_m}||_\infty)$

Now, taking the summation over $g = 0, ..., G_m - 1$ provides the following

$$\begin{aligned}&\sum_{t\in\mathcal{G}_m}\left(V_t^* - V_t^{\pi_t}\right)\\ =&(\gamma+2)C'\frac{1-(1-\eta\tau)^{G_m}}{\eta\tau} + G_m\cdot\left(\frac{2(\gamma+2)}{1-\gamma}\left(1+\frac{\gamma}{\eta\tau}\right)\cdot\epsilon_f + \frac{2\tau\log|\mathcal{A}|}{1-\gamma}\right)\\ &+\frac{1-\gamma^H}{1-\gamma}\cdot\left(\sum_{g=0}^{G_m-1}B_r(t_m+g, t_m+G_m-1)\right) + \frac{\gamma}{1-\gamma}\cdot\left(\frac{1-\gamma^H}{1-\gamma} - \gamma^{H-1}H\right)\cdot\left(\sum_{g=0}^{G_m-1}B_p(t_m+g, t_m+G_m-1)\right)\\ &+\frac{1-\gamma^H}{1-\gamma}\left(\sum_{g=0}^{G_m-1}B_r(t_m+g, t_m+G_m-1) + \frac{r_{max}}{1-\gamma}\sum_{g=0}^{G_m-1}B_p(t_m+g, t_m+G_m-1)\right)\\ \leq&(\gamma+2)C'\frac{1-(1-\eta\tau)^{G_m}}{\eta\tau} + G_m\cdot\left(\frac{2(\gamma+2)}{1-\gamma}\left(1+\frac{\gamma}{\eta\tau}\right)\cdot\epsilon_f + \frac{2\tau\log|\mathcal{A}|}{1-\gamma}\right)\\ &+\frac{2(1-\gamma^H)}{1-\gamma}\cdot\left(\bar{B}_r(t_m, t_m+G_m-1)\right) + \left(\frac{\gamma}{1-\gamma}\cdot\left(\frac{1-\gamma^H}{1-\gamma} - \gamma^{H-1}H\right) + \frac{1-\gamma^H}{1-\gamma}\cdot\frac{r_{max}}{1-\gamma}\right)\cdot\left(\bar{B}_r(t_m, t_m+G_m-1)\right)\\ &=\frac{C_1}{\eta\tau}\cdot\left(1-(1-\eta\tau)^{G_m}\right) + G_m\cdot(C_2\epsilon_f + C_3) + C_4\bar{B}_r(\mathcal{G}_m) + C_5\bar{B}_p(\mathcal{G}_m)\end{aligned}$$

where $C_1 = (\gamma+2)\left(||Q_{t_m}^* - Q_{t_m}||_\infty + 2\tau(1-\frac{\eta\tau}{1-\gamma}||\log\pi_{t_m}^* - \log\pi_{t_m}||_\infty)\right), C_2 = \frac{2(\gamma+2)}{1-\gamma}\left(1+\frac{\gamma}{\eta\tau}\right), C_3 = \frac{2\tau\log|\mathcal{A}|}{1-\gamma}, C_4 = \frac{2(1-\gamma^H)}{1-\gamma}, C_5 = \frac{\gamma}{1-\gamma}\cdot\left(\frac{1-\gamma^H}{1-\gamma} - \gamma^{H-1}H\right) + \frac{1-\gamma^H}{1-\gamma}\cdot\frac{r_{max}}{1-\gamma}$ □

Proof of Lemma 5.2. The policy hold error can be divided into three terms

$$\begin{aligned}\sum_{t\in\mathcal{N}_m}(V_t^* - V_t^{\pi_t}) &= \sum_{n=0}^{N_m-1}(V_{t_m+G_m+n}^* - V_{t_m+G_m+n}^{\pi_{t_m+G_m}})\\ &= \sum_{n=0}^{N_m-1}\left(\underbrace{(V_{t_m+G_m+n}^* - V_{t_m+G_m}^*)}_{\text{(2-I)}} + \underbrace{(V_{t_m+G_m}^* - V_{t_m+G_m}^{\pi_{t_m+G_m}})}_{\text{(2-II)}} + \underbrace{(V_{t_m+G_m}^{\pi_{t_m+G_m}} - V_{t_m+G_m+n}^{\pi_{t_m+G_m}})}_{\text{2-III}}\right)\end{aligned}$$

The terms (2-I), (2-II) and (2-III) can be bounded using Corollary D.3, Lemma D.1 and Lemma D.4. Recall that we have defined the time interval $\mathcal{N}_m = [t_m + G_m, t_{m+1})$ where $t_{m+1} = t_m + G_m + N_m$.

- $V_{t_m+G_m+n}^* - V_{t_m+G_m}^* \leq \frac{1-\gamma^H}{1-\gamma}\left(B_r(t_m+G_m, t_m+G_m+n) + \frac{r_{max}}{1-\gamma}B_p(t_m+G_m, t_m+G_m+n)\right)$
- $V_{t_m+G_m}^* - V_{t_m+G_m}^{\pi_{t_m+G_m}} \leq (\gamma+2)((1-\eta\tau)^{G_m}C') + \frac{2(\gamma+2)}{1-\gamma}\left(1+\frac{\gamma}{\eta\tau}\right)\cdot\epsilon_f + \frac{2\tau\log|\mathcal{A}|}{1-\gamma}$
- $V_{t_m+G_m}^{\pi_{t_m+G_m}} - V_{t_m+G_m+n}^{\pi_{t_m+G_m}} \leq \frac{1-\gamma^H}{1-\gamma}\cdot B_r(t_m+G_m, t_m+G_m+n) + \frac{\gamma}{1-\gamma}\cdot\left(\frac{1-\gamma^H}{1-\gamma} - \gamma^{H-1}H\right)\cdot B_p(t_m+G_m, t_m+G_m+n)$

Now taking summation over $n = 0, 1, ..., N_m - 1$ provides the following.

$$\begin{aligned}&\sum_{t\in\mathcal{N}_m}(V_t^* - V_t^{\pi_t})\\ =&N_m\cdot\left((\gamma+2)((1-\eta\tau)^{G_m}C') + \frac{2(\gamma+2)}{1-\gamma}\left(1+\frac{\gamma}{\eta\tau}\right)\cdot\epsilon_f + \frac{2\tau\log|\mathcal{A}|}{1-\gamma}\right)\\ &+\frac{1-\gamma^H}{1-\gamma}\cdot\left(\sum_{n=0}^{N_m-1}B_r(t_m+G_m, t_m+G_m+n)\right) + \frac{\gamma}{1-\gamma}\cdot\left(\frac{1-\gamma^H}{1-\gamma} - \gamma^{H-1}H\right)\cdot\left(\sum_{n=0}^{N_m-1}B_p(t_m+G_m, t_m+G_m+n)\right)\\ &+\frac{1-\gamma^H}{1-\gamma}\left(\sum_{n=0}^{N_m-1}B_r(t_m+G_m, t_m+G_m+n) + \frac{r_{max}}{1-\gamma}\sum_{n=0}^{N_m-1}B_p(t_m+G_m, t_m+G_m+n)\right)\\ \leq&N_m\cdot\left((\gamma+2)((1-\eta\tau)^{G_m}C') + \frac{2(\gamma+2)}{1-\gamma}\left(1+\frac{\gamma}{\eta\tau}\right)\cdot\epsilon_f + \frac{2\tau\log|\mathcal{A}|}{1-\gamma}\right)\\ &+\frac{2(1-\gamma^H)}{1-\gamma}\cdot\left(\bar{B}_r(t_m+G_m, t_m+G_m+N_m-1)\right)\\ &+\left(\frac{\gamma}{1-\gamma}\cdot\left(\frac{1-\gamma^H}{1-\gamma} - \gamma^{H-1}H\right) + \frac{1-\gamma^H}{1-\gamma}\cdot\frac{r_{max}}{1-\gamma}\right)\cdot\left(\bar{B}_r(t_m+G_m, t_m+G_m+N_m-1)\right)\\ =&N_m\cdot\left(C_1(1-\eta\tau)^{G_m} + C_2\epsilon_f + C_3\right) + C_4\bar{B}_r(\mathcal{N}_m) + C_5\bar{B}_p(\mathcal{N}_m)\end{aligned}$$

where C_1, C_2, C_3, C_4, C_5 are the constants that we defined in the Lemma 5.1. □

Proof of Theorem 5.3. Note that the following relationship holds for dynamic regret $\mathfrak{R}(T)$

$$\mathfrak{R}(T) = \sum_{m=1}^{M}\left(\underbrace{\sum_{t\in\mathcal{G}_m}(V_t^* - V_t^{\pi_t})}_{\text{Policy update error}} + \underbrace{\sum_{t\in\mathcal{N}_m}(V_t^* - V_t^{\pi_t})}_{\text{Policy hold error}}\right).$$

Use Lemma 5.1 to upper bound the policy update error and Lemma 5.2 to upper bound the policy hold error. Then, it holds that

$$
\begin{aligned}
\mathfrak{R}(T) &= \sum_{m=1}^{M} \left(\sum_{t \in \mathcal{G}_m} (V_t^* - V_t^{\pi_t}) + \sum_{t \in \mathcal{N}_m} (V_t^* - V_t^{\pi_t}) \right) \\
&\leq \sum_{m=1}^{M} \left(\frac{C_1}{\eta\tau} \cdot \Big(1 - (1-\eta\tau)^{G_m}\Big) + G_m \Big(C_2 \delta_m^f + C_3\Big) + C_4 \bar{B}_r(\mathcal{G}_m) + C_5 \bar{B}_p(\mathcal{G}_m) \right. \\
&\left. + N_m \cdot \Big(C_1(1-\eta\tau)^{G_m} + C_2\delta_m^f + C_3\Big) + C_4 \bar{B}_r(\mathcal{N}_m) + C_5 \bar{B}_p(\mathcal{N}_m) \right) \\
&= \sum_{m=1}^{M} \left(\frac{C_1}{\eta\tau} + \left(N_m C_1 - \frac{C_1}{\eta\tau} \right) (1-\eta\tau)^{G_m} + (N_m + G_m)(C_2 \delta_m^f + C_3) + \bar{B}(t_m, t_{m+1}) \right)
\end{aligned}
$$

□

Proof of Lemma 5.4. Refer to the proof of Theorem 5.8. □

Proof of Proposition 5.6. For fixed t_m, t_{m+1}, note that $\bar{B}(t_m, t_{m+1})$ is a function of G_m, N_m with a constraint $G_m + N_m = t_{m+1} - t_m$. In this proof, we let $\bar{B}(t_m, t_{m+1})$ to be denoted as a function $g(G_m, N_m)$. Recall that we have defined $\bar{B}(t_{m+1}, t_m) := \bar{B}(\mathcal{N}_m) + \bar{B}(\mathcal{G}_m)$. Now, since $g(0, t_{m+1} - t_m) = g(t_{m+1} - t_m, 0) = \sum_{t=t_m}^{t_{m+1}-1} (C_4 B_r(t_m, t) + C_5 B_p(t_m, t))$, it is sufficient to show the existence of $G_m^\dagger \in (0, t_{m+1}, t_m)$ and $N_m^\dagger \in (0, t_{m+1}, t_m)$ that satisfy $g(G_m^\dagger, N_m^\dagger) < g(0, t_{m+1} - t_m) = g(t_{m+1} - t_m, 0)$. By the definition of non-stationary environment (see Definition 3.4), let $t_1^\dagger, t_2^\dagger$ satisfy $B_r(t_1^\dagger, t_2^\dagger) > 0$ or $B_p(t_1^\dagger, t_2^\dagger) > 0$. Now, letting $G_m^\dagger = t_2^\dagger$, then we have $B_r(t_m, G_m^\dagger) > 0$ or $B_p(t_m, G_m^\dagger) > 0$. Then we could say that $\sum_{t_m}^{t_m + G_m^\dagger - 1} B_r(t_m, t) + \sum_{t_m + G_m^\dagger}^{t_{m+1}-1} B_r(t_m + G_m^\dagger, t) < \sum_{t_m}^{t_{m+1}-1} B_r(t_m, t)$ or $\sum_{t_m}^{t_m + G_m^\dagger - 1} B_p(t_m, t) + \sum_{t_m + G_m^\dagger}^{t_{m+1}-1} B_p(t_m + G_m^\dagger, t) < \sum_{t_m}^{t_{m+1}-1} B_p(t_m, t)$ hold. Now, by combining two inequalities with constants $C_4, C_5 > 0$ defined in Lemma 5.1, we have the following.

$$
\begin{aligned}
&C_4 \bar{B}_r(t_m, t_m + G_m^\dagger) + C_4 \bar{B}_r(t_m + G_m^\dagger, T_{m+1}) + C_5 \bar{B}_p(t_m, t_m + G_m^\dagger) + C_5 \bar{B}_p(t_m + G_m^\dagger, t_{m+1}) \\
&< C_4 \bar{B}_r(t_m, t_{m+1}) + C_5 \bar{B}_p(t_m, t_{m+1})
\end{aligned}
$$

$\Leftrightarrow$

$$
\bar{B}(t_m, t_m + G_m^\dagger) + \bar{B}(t_m + G_m^\dagger, t_{m+1}) < \bar{B}(t_m, t_{m+1})
$$

Therefore, $G_m^\dagger = t_2^\dagger, N_m^\dagger = t_{m+1} - t_m - t_m^\dagger$ satisfies condition $g(G_m^\dagger, N_m^\dagger) < g(0, t_{m+1} - t_m) = g(t_{m+1} - t_m, 0)$. This completes the proof. □

Proof of Theorem 5.8. We first show that the policy optimization error is a convex function of G_m (or N_m. Let $f_1(N_m, G_m) = C_1(1 - (1-\eta\tau)^{G_m}) + N_m C_1 (1-\eta\tau)^{G_m}$ where $N_m + G_m = t_{m+1} - t_m$ is a constant. Note that $\partial N_m / \partial G_m = -1$.

$$
\frac{1}{C_1} \cdot \frac{\partial f_1}{\partial G_m} = \big\{ \ln(1-\eta\tau)\,(N_m - 1) - 1 \big\} (1-\eta\tau)^{G_m}
$$

and

$$
\frac{1}{C_1} \cdot \frac{\partial^2 f_1}{\partial G_m^2} = \big\{ (\ln(1-\eta\tau))^2 (N_m - 1) - 2\ln(1-\eta\tau) \big\} (1-\eta\tau)^{G_m}
$$

Therefore $\partial^2 f_1 / \partial G_m^2 > 0$ and $\partial^2 f_1 / \partial N_m^2 > 0$ holds for $\forall N_m, G_m \geq 0$ where $N_m + G_m = t_{m+1} - t_m$ holds. The non-stationary terms are bounded as follows.

$$
\bar{B}(\mathcal{N}_m) + \bar{B}(\mathcal{G}_m) = (C_4 + C_5) \left(\bar{B}_r(\mathcal{N}_m) + \bar{B}_r(\mathcal{G}_m) \right)
$$

Note that by Assumption 3.1, $\bar{B}_r(\mathcal{N}_m) \leq \sum_{t=t_m+G_m}^{t=t_m+G_m+N_m-1} \alpha_r^{t-(t_m+G_m)} B^{\max}(\mathcal{N}_m)$ and $\bar{B}_r(\mathcal{G}_m) \leq \sum_{t=t_m}^{t=t_m+G_m-1} \alpha_r^{t-t_m} B^{\max}(\mathcal{G}_m)$. For the short notation, we use $\alpha_\diamond(\mathcal{G}_m) = \alpha_{\diamond,1}, \alpha_\diamond(\mathcal{N}_m) = \alpha_{\diamond,2}$ and $B^{\max}_\diamond(\mathcal{G}_m) = B^{\max}_{\diamond,1}, B^{\max}_\diamond(\mathcal{N}_m) = B^{\max}_{\diamond,2}$ where $\diamond = r$ or p. Also, we let $\alpha_\square = \max(\alpha_{r,\square}, \alpha_{p,\square})$ and $B^{\max}_\square = \max(B^{\max}_{r,\square}, B^{\max}_{p,\square})$ where $\square = 1$ or 2. Then the upper bound would be

$$\begin{aligned}\bar{B}(\mathcal{N}_m) + \bar{B}(\mathcal{G}_m) &= C_4\left(\bar{B}_r(\mathcal{N}_m) + \bar{B}_r(\mathcal{G}_m)\right) + C_5\left(\bar{B}_p(\mathcal{N}_m) + \bar{B}_p(\mathcal{G}_m)\right) \\ &\leq (C_4 + C_5) \cdot \left(\frac{\alpha_1^{G_m} - 1}{\alpha_1 - 1} \cdot B_1^{\max} + \frac{\alpha_2^{N_m} - 1}{\alpha_2 - 1} \cdot B_2^{\max}\right)\end{aligned}$$

We denote the upper bound as a function $f_2(N_m, G_m)$. Note that if $B_1^{\max}, B_2^{\max} > 0$ for a non-stationary environment. Also, if $0 < \alpha_1, \alpha_2 < 1$, then $f_2(N_m, G_m)$ is a concave function with respect to (N_m, G_m) and if $\alpha_1, \alpha_2 > 1$, then $f_2(N_m, G_m)$ is a convex function with respect to (N_m, G_m). □

D. Supplementary lemmas

Lemma D.1 (NPG Convergence)**.** *Assume that we have inexact Q value estimation at time $t_m + G_m - 1$, $\hat{Q}_{t_m+G_m-1}$ where we denote $Q_{t_m+G_m-1}$ as the exact Q value. Now, define the error of estimation as ϵ, that is, $||Q_{t_m+G_m-1} - \hat{Q}_{t_m+G_m-1}||_\infty \leq \epsilon_f$. For any $g \in [G_m]$, it holds that*

$$V^*_{t_m+G_m-1} - V^{\pi^g}_{t_m+G_m-1} \leq (\gamma+2)((1-\eta\tau)^{g-1}C_1) + \frac{2(\gamma+2)}{1-\gamma}\left(1 + \frac{\gamma}{\eta\tau}\right) \cdot \epsilon_f + \frac{2\tau \log|\mathcal{A}|}{1-\gamma}$$

where

$$C_1 = \left|\left|Q_\tau^* - Q_\tau^{(0)}\right|\right|_\infty + 2\tau\left(1 - \frac{n\tau}{1-\gamma}\right)\left|\left|\log \pi_\tau^* - \log \pi^{(0)}\right|\right|_\infty$$

Proof of Lemma D.1. We omit the underscript t for simplicity of notation, i.e., $V_t, V_{\tau,t}, V_t^*$ denotes V, V_τ, V^*, respectively. For any $m \in [M]$ and any $t \in \mathcal{G}_m$,

$$\begin{aligned}V^*(s) - V(s) &\leq ||V^*(\cdot) - V_\tau^*(\cdot)||_\infty + ||V_\tau^*(\cdot) - V_\tau(\cdot)||_\infty + ||V_\tau(\cdot) - V(\cdot)||_\infty \\ &\leq ||V_\tau^*(\cdot) - V_\tau(\cdot)||_\infty + \frac{2\tau \log|\mathcal{A}|}{1-\gamma}\end{aligned}$$

holds, since for any policy π, $||V_\tau^\pi - V^\pi||_\infty = \tau \max_s |\mathcal{H}(s,\pi)| \leq \frac{\tau \log|\mathcal{A}|}{1-\gamma}$ holds. Now, note that V_τ is a value function of a policy π_τ that we obtain after updating g iterations.

$$\begin{aligned}||V_\tau^*(\cdot) - V_\tau(\cdot)||_\infty &\leq \tau\, ||\log \pi_\tau^* - \log \pi_\tau^g||_\infty + ||Q_\tau^*(\cdot) - Q_\tau(\cdot)||_\infty \\ &\leq \tau \cdot \frac{2}{\tau}\left((1-\eta\tau)^{g-1}C_1 + C_2\right) + \gamma\left((1-\eta\tau)^{g-1}C_1 + C_2\right) \qquad (2) \\ &= (\gamma+2)\left((1-\eta\tau)^{g-1}C_1 + C_2\right)\end{aligned}$$

where

$$C_1 = \left|\left|Q_\tau^* - Q_\tau^{(0)}\right|\right|_\infty + 2\tau\left(1 - \frac{n\tau}{1-\gamma}\right)\left|\left|\log \pi_\tau^* - \log \pi^{(0)}\right|\right|_\infty,\ C_2 = \frac{2\epsilon_f}{1-\gamma}\left(1 + \frac{\gamma}{\eta\tau}\right)$$

. Equation 2 holds by Theorem 2 of (Cen et al., 2022). □

Lemma D.2 (Difference between optimal state action value functions of two MDPs)**.** *For any two time steps $t_1, t_2 \in T$, we denote the optimal Q functions at step $h \in [H]$ as $Q^*_{t_1,h}(s,a), Q^*_{t_2,h}(s,a)$. Then for any state and action pair $s, a \in \mathcal{S} \times \mathcal{A}$,*

$$Q^*_{t_1,h}(s,a) - Q^*_{t_2,h}(s,a) \leq \sum_{h'=h}^{H-1} \gamma^{h'-h} B_r(t_1,t_2) + \frac{r_{max}}{1-\gamma}\sum_{h'=h}^{H-1} \gamma^{h'-h} B_p(t_1,t_2)$$

holds where $B_r(t_1,t_2), B_p(t_1,t_2)$ denotes local time-elapsing variation budget between timesteps $\{t_1, t_1+1, t_1+2, ..., t_2\}$.

Proof of Lemma D.2. Only for the purpose of the proof of Lemma D.2, we define the state value function $V^\pi_{t,h} : \mathcal{S} \to \mathbb{R}$ and the state action value function $Q^\pi_{t,h} : \mathcal{S} \times \mathcal{A} \to \mathbb{R}$ at step h of time t as

$$V^\pi_{t,h}(s) := \mathbb{E}_{\mathcal{M}_t}\left[\sum_{h'=h}^{H-1} \gamma^{h'-h} r_{t,h'} \,\middle|\, s^0_t = s\right]$$

and

$$Q^\pi_{t,h}(s,a) := \mathbb{E}_{\mathcal{M}_t}\left[\sum_{h'=h}^{H-1} \gamma^{h'-h} r_{t,h'} \,\middle|\, s^0_t = s, a^0_t = a\right].$$

Note that the optimal state value function and the state action value function satisfy the following Bellman equation.

$$Q^*_{t,h}(s,a) = \left(R_{t,h} + \gamma P_t V^*_{t,h}\right)(s,a), \pi^*_t = \arg\max_{a \in \mathcal{A}} Q^*_{t,h}(s,a)$$

The proof depends on backward induction. First, the statement holds when $h = H-1$ since

$$\left|\left|Q^*_{t_1,H-1}(s,a) - Q^*_{t_2,H-1}(s,a)\right|\right|_\infty = ||r_{t_1,H-1} - r_{t_2,H-1}||_\infty = ||R_{t_1} - R_{t_2}||_\infty$$

holds. Now, we assume that the statement of Lemma D.2 holds when $h+1$. Then, when h,

$$\begin{aligned}
Q^*_{t_1,h}(s,a) - Q^*_{t_2,h}(s,a) &= \left(R_{t_1,h} - R_{t_2,h}\right)(s,a) + \gamma \sum_{s' \in \mathcal{S}} \Big(P_{t_1}(s'|s,a) V^*_{t_1,h+1}(s') - P_{t_2}(s'|s,a) V^*_{t_2,h+1}(s')\Big) \\
&\le B_r(t_1,t_2) + \gamma \sum_{s' \in \mathcal{S}} \Big(P_{t_1}(s'|s,a) Q^*_{t_1,h+1}(s', \pi^*_{t_1}(s')) - P_{t_2}(s'|s,a) Q^*_{t_2,h+1}(s', \pi^*_{t_2}(s')(s')\Big)
\end{aligned}$$

Then by the induction hypothesis on $h+1$, the following holds for any $s' \in \mathcal{S}$.

$$\begin{aligned}
Q^*_{t_1,h+1}(s', \pi^*_{t_1}(s')) &\le Q^*_{t_2,h+1}(s', \pi^*_{t_1}(s')) + \sum_{h'=h+1}^{H-1} \gamma^{h'-(h+1)} B_r(t_1,t_2) + \frac{r_{\max}}{1-\gamma} \sum_{h'=h+1}^{H-1} \gamma^{h'-(h+1)} B_p(t_1,t_2) \\
&\le Q^*_{t_2,h+1}(s', \pi^*_{t_2}(s')) + \sum_{h'=h+1}^{H-1} \gamma^{h'-(h+1)} B_r(t_1,t_2) + \frac{r_{\max}}{1-\gamma} \sum_{h'=h+1}^{H-1} \gamma^{h'-(h+1)} B_p(t_1,t_2)
\end{aligned}$$

Then we have the following.

$$\begin{aligned}
Q^*_{t_1,h}(s,a) - Q^*_{t_2,h''}(s,a) &\le B_r(t_1,t_2) + \gamma \sum_{s' \in \mathcal{S}} \Big(\Big(P_{t_1}(s'|s,a) - P_{t_2}(s'|s,a)\Big) Q^*_{t_2,h+1}(s', \pi^*_{t_2}(s'))\Big) \\
&\quad + \sum_{h'=h+1}^{H-1} \gamma^{h'-h} B_r(t_1,t_2) + \frac{r_{\max}}{1-\gamma} \sum_{h'=h+1}^{H-1} \gamma^{h'-h} B_p(t_1,t_2) \\
&\le \gamma \Big|\Big|\Big(P_{t_1}(s'|s,a) - P_{t_2}(s'|s,a)\Big|\Big|_1 \left|\left|Q^*_{t_2,h+1}(s', \pi^*_{t_2}(s'))\right|\right|_\infty + \sum_{h'=h}^{H-1} \gamma^{h'-h} B_r(t_1,t_2) \\
&\quad + \frac{r_{\max}}{1-\gamma} \sum_{h'=h+1}^{H-1} \gamma^{h'-h} B_p(t_1,t_2) \\
&\le \gamma B_p(t_1,t_2) \cdot \frac{r_{max}}{1-\gamma} + \sum_{h'=h}^{H-1} \gamma^{h'-h} B_r(t_1,t_2) + \frac{r_{\max}}{1-\gamma} \sum_{h'=h+1}^{H-1} \gamma^{h'-h} B_p(t_1,t_2) \\
&= \sum_{h'=h}^{H-1} \gamma^{h'-h} B_r(t_1,t_2) + \frac{r_{\max}}{1-\gamma} \sum_{h'=h}^{H-1} \gamma^{h'-h} B_p(t_1,t_2)
\end{aligned}$$

This completes the proof. □

Corollary D.3 (Difference between optimal state value functions of two MDPs)**.** *For any two time $t_1 < t_2 \in T$, we gap between two value functions at time t_1 and t_2 is bounded as*

$$||V^*_{t_1}(s) - V^*_{t_2}(s)||_\infty \leq \frac{1-\gamma^H}{1-\gamma}\left(B_r(t_1,t_2) + \frac{r_{max}}{1-\gamma}B_p(t_1,t_2)\right)$$

Proof of Corollary D.3. Corollary D.3 comes from Lemma D.2. □

Lemma D.4 (Difference between value functions of two MDPs with same policy)**.** *For any two time $t_1, t_2 \in T$, any policy π, and any state $s \in \mathcal{S}$, the gap between two value functions $V^\pi_{t_1}$ and $V^\pi_{t_2}$ is bounded as follows.*

$$V^\pi_{t_1}(s) - V^\pi_{t_2}(s) \leq \frac{1-\gamma^H}{1-\gamma}\cdot B_r(t_1,t_2) + \frac{\gamma}{1-\gamma}\cdot\left(\frac{1-\gamma^H}{1-\gamma} - \gamma^{H-1}H\right)\cdot B_p(t_1,t_2)$$

Proof of Lemma D.4. For given initial state s_0, we first define the occupancy measure of state and action (s, a) as

$$\rho^\pi_t(s,a) := \sum_{h=0}^{H-1}\gamma^h\mathbb{P}\left(s_h = s, a_h = a|P_t,\pi\right).$$

It is worth noting that $\mathbb{P}\left(s_h = s, a_h = a|P_t,\pi\right) = \mathbb{P}\left(s_h = s|P_t,\pi\right)\cdot\pi(a_h = a|s_s = s)$. Now, note that the value function can be rewritten using the occupancy measure as

$$V^\pi_t(s) := \mathbb{E}_{\mathcal{M}_t}\left[\sum_{h=0}^{H-1}\gamma^h r_{t,h} \mid s^0_t = s\right] = \mathbb{E}_{(s,a)\sim\rho^\pi_t}\left[R_t(s,a)\right]$$

Then for any $t_1, t_2 \in T$, the gap between two value functions are expressed as

$$\begin{aligned}
V^\pi_{t_1}(s) - V^\pi_{t_2}(s) &= \mathbb{E}_{(s,a)\sim d^\pi_{t_1}}\left[R_{t_1}(s,a)\right] - \mathbb{E}_{(s,a)\sim d^\pi_{t_2}}\left[R_{t_2}(s,a)\right]\\
&= \mathbb{E}_{(s,a)\sim d^\pi_{t_1}}\left[R_{t_1}(s,a) - R_{t_2}(s,a)\right] - \mathbb{E}_{(s,a)\sim d^\pi_{t_1}}\left[R_{t_2}(s,a)\right] + \mathbb{E}_{(s,a)\sim d^\pi_{t_2}}\left[R_{t_2}(s,a)\right]\\
&\leq \frac{1-\gamma^H}{1-\gamma}\cdot\max_{(s,a)}\left(|R_{t_2}(s,a) - R_{t_1}(s,a)|\right) + \left(\mathbb{E}_{(s,a)\sim d^\pi_{t_2}}\left[R_{t_2}(s,a)\right] - \mathbb{E}_{(s,a)\sim d^\pi_{t_1}}\left[R_{t_2}(s,a)\right]\right)\\
&= \frac{1-\gamma^H}{1-\gamma}\cdot B_r(t_1,t_2) + \left(\mathbb{E}_{(s,a)\sim d^\pi_{t_2}}\left[R_{t_2}(s,a)\right] - \mathbb{E}_{(s,a)\sim d^\pi_{t_1}}\left[R_{t_2}(s,a)\right]\right) \qquad (3)
\end{aligned}$$

Now, the gap $\mathbb{E}_{(s,a)\sim d^\pi_{t_2}}\left[R_{t_2}(s,a)\right] - \mathbb{E}_{(s,a)\sim d^\pi_{t_1}}\left[R_{t_2}(s,a)\right]$ is upper bounded as follows.

$$\begin{aligned}
\mathbb{E}_{(s,a)\sim d^\pi_{t_2}}\left[R_{t_2}(s,a)\right] - \mathbb{E}_{(s,a)\sim d^\pi_{t_1}}\left[R_{t_2}(s,a)\right] &\leq ||\rho^\pi_{t_2}(\cdot,\cdot) - \rho^\pi_{t_1}(\cdot,\cdot)||_1\cdot||R_{t_2}(\cdot,\cdot)||_\infty\\
&= ||\rho^\pi_{t_2}(\cdot,\cdot) - \rho^\pi_{t_1}(\cdot,\cdot)||_1\cdot r_{\text{max}}. \qquad (4)
\end{aligned}$$

Now, the term $\sum_{(s,a)} |\rho^{\pi}_{t_2}(s,a) - \rho^{\pi}_{t_1}(s,a)|$ is bounded as follows.

$$\begin{aligned}
\sum_{(s,a)} \left|\rho^{\pi}_{t_2}(s,a) - \rho^{\pi}_{t_1}(s,a)\right| &= \sum_{(s,a)} \left| \sum_{h=0}^{H-1} \Big(\gamma^h \cdot \big(\mathbb{P}\left(s_h = s|P_{t_2}, \pi\right) - \mathbb{P}\left(s_h = s|P_{t_1}, \pi\right)\big) \cdot \pi(a_h = a|s_h = s) \Big) \right| \\
&= \sum_{(s,a)} \left(\sum_{h=0}^{H-1} \left|\gamma^h \cdot \big(\mathbb{P}\left(s_h = s|P_{t_2}, \pi\right) - \mathbb{P}\left(s_h = s|P_{t_1}, \pi\right)\big)\right| \cdot \left|\pi(a_h = a|s_h = s)\right| \right) \\
&= \sum_{s} \left(\sum_{h=0}^{H-1} \left|\gamma^h \cdot \big(\mathbb{P}\left(s_h = s|P_{t_2}, \pi\right) - \mathbb{P}\left(s_h = s|P_{t_1}, \pi\right)\big)\right| \cdot \sum_{a \in \mathcal{A}} \left|\pi(a_h = a|s_h = s)\right| \right) \\
&= \sum_{s \in \mathcal{S}} \left(\sum_{h=0}^{H-1} \left|\gamma^h \cdot \big(\mathbb{P}\left(s_h = s|P_{t_2}, \pi\right) - \mathbb{P}\left(s_h = s|P_{t_1}, \pi\right)\big)\right| \cdot 1 \right) \\
&= \sum_{h=0}^{H-1} \gamma^h \cdot \left(\sum_{s \in \mathcal{S}} \left| \big(\mathbb{P}\left(s_h = s|P_{t_2}, \pi\right) - \mathbb{P}\left(s_h = s|P_{t_1}, \pi\right)\big) \right| \right). \qquad (5)
\end{aligned}$$

Now, for simplicity of notation, we denote $\mathbb{P}(s_h = s|P_t, \pi)$ as $\mathbb{P}^h_t(s)$, $P_t(s_h = s|s_{h-1} = s', a_{h-1} = a')$ as $\mathbb{P}^h_t(s|s', a')$, and $\pi(a_h = a|s_h = s)$ as $\pi^h(a|s)$. Then, we have

$$\begin{aligned}
&\sum_{s \in \mathcal{S}} \left|\mathbb{P}^h_{t_2}(s) - \mathbb{P}^h_{t_1}(s)\right| \\
&= \sum_{s \in \mathcal{S}} \left| \sum_{s', a'} \left(P^h_{t_2}(s|s', a') \cdot \pi^{h-1}(a'|s') \cdot \mathbb{P}^{h-1}_{t_2}(s') - P^h_{t_1}(s|s', a') \cdot \pi^{h-1}(a'|s') \cdot \mathbb{P}^{h-1}_{t_1}(s') \right) \right| \\
&\leq \sum_{s \in \mathcal{S}} \sum_{s', a'} \left| \left(P^h_{t_2}(s|s', a') \cdot \mathbb{P}^{h-1}_{t_2}(s') - P^h_{t_1}(s|s', a') \cdot \mathbb{P}^{h-1}_{t_1}(s') \right) \cdot \pi^{h-1}(a'|s') \right| \\
&= \sum_{s', a'} \sum_{s \in \mathcal{S}} \left| \left(P^h_{t_2}(s|s', a') \cdot \mathbb{P}^{h-1}_{t_2}(s') - P^h_{t_1}(s|s', a') \cdot \mathbb{P}^{h-1}_{t_1}(s') \right) \cdot \pi^{h-1}(a'|s') \right| \\
&\leq \sum_{s', a'} \sum_{s \in \mathcal{S}} \left(\left| \big(P^h_{t_2}(s|s', a') - P^h_{t_1}(s|s', a')\big) \cdot \mathbb{P}^{h-1}_{t_2}(s') \cdot \pi^{h-1}(a'|s') \right| + \left| \big(\mathbb{P}^{h-1}_{t_2}(s') - \mathbb{P}^{h-1}_{t_1}(s')\big) \cdot P^h_{t_1}(s|s', a') \cdot \pi^{h-1}(a'|s') \right| \right) \\
&\leq \max_{s', a'} \big(||P^h_{t_2}(\cdot|s', a') - P^h_{t_1}(\cdot|s', a')||_1 \big) \cdot \left(\sum_{s', a'} \big(\mathbb{P}^{h-1}_{t_2}(s') \cdot \pi^{h-1}(a'|s') \big) \right) \\
&\qquad + \left(\sum_{s', a'} \big(\left|\mathbb{P}^{h-1}_{t_2}(s') - \mathbb{P}^{h-1}_{t_1}(s')\right| \big) \cdot \pi^{h-1}(a'|s') \right) \cdot \left(\sum_{s \in \mathcal{S}} P^h_{t_1}(s|s', a') \right) \\
&= B_p(t_1, t_2) \cdot \left(\sum_{s' \in \mathcal{S}} \mathbb{P}^{h-1}_{t_2}(s') \cdot \sum_{a' \in \mathcal{A}} \pi^{h-1}(a'|s') \right) + \left(\sum_{s' \in \mathcal{S}} \left|\mathbb{P}^{h-1}_{t_2}(s') - \mathbb{P}^{h-1}_{t_1}(s')\right| \cdot \sum_{a' \in \mathcal{A}} \pi^{h-1}(a'|s') \right) \cdot 1 \\
&= B_p(t_1, t_2) + \sum_{s' \in \mathcal{S}} \left|\mathbb{P}^{h-1}_{t_2}(s') - \mathbb{P}^{h-1}_{t_1}(s')\right|.
\end{aligned}$$

Now, note that $\sum_{s \in \mathcal{S}} \left|\mathbb{P}^0_{t_2}(s) - \mathbb{P}^0_{t_1}(s)\right| = 0$ and $\sum_{s \in \mathcal{S}} \left|\mathbb{P}^1_{t_2}(s) - \mathbb{P}^1_{t_1}(s)\right| = B_p(t_1, t_2)$ holds. Therefore,

$$\sum_{s \in \mathcal{S}} \left|\mathbb{P}^h_{t_2}(s) - \mathbb{P}^h_{t_1}(s)\right| \leq h B_p(t_1, t_2)$$

holds. Then, putting the above inequality in the inequality (5) gives the following.

$$\begin{aligned}\sum_{(s,a)} \left|\rho^{\pi}_{t_2}(s,a) - \rho^{\pi}_{t_1}(s,a)\right| &\leq \sum_{h=0}^{H-1} \gamma^h h B_p(t_1,t_2) \\ &\leq \frac{\gamma}{1-\gamma} \cdot \left(\frac{1-\gamma^H}{1-\gamma} - \gamma^{H-1} H\right) \cdot B_p(t_1,t_2)\end{aligned}$$

Now, plugging in the above inequality into the inequalities (3) and (4) provides the following.

$$V^{\pi}_{t_1}(s) - V^{\pi}_{t_2}(s) \leq \frac{1-\gamma^H}{1-\gamma} \cdot B_r(t_1,t_2) + \frac{\gamma}{1-\gamma} \cdot \left(\frac{1-\gamma^H}{1-\gamma} - \gamma^{H-1} H\right) \cdot B_p(t_1,t_2)$$

□

E. Experiment Platforms and Licenses

E.1. Platforms

All experiments are conducted on 12 Intel Xeon CPU E5-2690 v4 and 2 Tesla V100 GPUs.

E.2. Licenses

We have used the following libraries/ repos for our Python codes:

- Pytorch (BSD 3-Clause "New" or "Revised" License).
- OpenAI Gym (MIT License).
- Numpy (BSD 3-Clause "New" or "Revised" License).
- Official codes distributed from *https://github.com/pranz24/pytorch-soft-actor-critic*: to compare the performance of SAC and FSAC in the Mujoco environment.
- Official codes distributed from the *https://github.com/linesd/tabular-methods*: to compare SAC and FSAC in the goal-switching cliff world.